Evaluation of performance of particulate Protein A affinity resins

University of Natural Resources
and Life Sciences, Vienna

Masterarbeit

Zur Erlangung des akademischen Grades
Diplom Ingenieur

Eingereicht von: **Andreas Daxbacher**
Matrikelnummer: **01541771**

An der **Universität für Bodenkultur**

Vorstand: **Univ.Prof. Dipl.-Ing. Dr.rer.nat. Reingard Grabherr**
Supervisor: **Assoc. Prof. Dipl.-Ing. Dr. Rainer Hahn**
Durchgeführt bei: **DBT, Universität für Bodenkultur**

Ehrenwörtliche Erklärung

Ich versichere hiermit,

1. dass ich die vorliegende Masterarbeit selbstständig verfasst, andere als die angegebenen Quellen und Hilfsmittel nicht benutzt und mich auch sonst keiner unerlaubten Hilfe bedient habe, sowie

2. dass ich diese Masterarbeit bisher weder im Inland noch im Ausland in irgendeiner Form als Prüfungsarbeit vorgelegt habe.

3. dass die in Papierform vorliegende Variante mit der digitalen Variante ident ist.

Einverständniserklärung

Ich erteile hiermit mein Einverständnis zur elektronischen Archivierung der vorliegenden Masterarbeit.

Wien, _____ _____

Unterschrift

Acknowledgements

I would first like to express great gratitude to my supervisor Rainer Hahn for giving me the opportunity to work, and write my master thesis in his working group. Further, I would like to thank him for his great scientific instructions, discussions and support throughout my work.

Furthermore, I would like to express great gratitude to the members of the working groups of AG Hahn and AG Jungbauer, which quickly admitted me and were building a great working environment. Especially I would like to acknowledge my colleges Mathias Kubek and Jürgen Beck for their helpfulness, support and scientific advice, especially at the beginning of my work.

I would like to express my gratitude to Sartorius which commission this study and supported me with high quality working material for my experiments.

Finally, I must express my very profound gratitude to my parents which facilitated my study, gave me great support throughout my educational path and encouraged me in the process of researching and writing this thesis.

Abstract:

The influence of velocity on process performance was investigated for two particulate Protein A affinity resins. MabSelect PrismA from GE Healthcare is a resin based on high-flow agarose and Toyopearl AF-rProtein A HC-650F has a polymethacrylate backbone. Both resins have recombinant Protein A ligands which are resistant to alkaline sanitization. The observed influence of velocity on dynamic binding capacity was expected and is also well documented in literature. In this thesis varying velocities were also tested for washing and elution steps with respect to host cell protein content and aggregation of a monoclonal antibody. However, this influence was rather small for the Toyopearl resins and negligible for MabSelect PrismA. Antibody aggregation could not be determined under any process conditions, even not for very harsh elution conditions. For Toyopearl, higher host cell protein content in eluates was determined when the column was operated at low protein saturation or higher velocities, which suggests interactions of host cell proteins primarily with the backbone. A washing step with a buffer solution containing isopropanol and urea yielded extremely low impurity levels for Toyopearl while it was only moderately effective for MabSelect PrismA. However, the impact of velocity on this removal was very small. Overall, the results of this study suggest that operating Protein A affinity media at high velocity does not affect host cell protein removal whereat the composition of the washing buffer is more important. These results are important in view of the new Protein A affinity membrane, which is currently under development at Sartorius.

Keywords:

mAb, protein A , influence of velocity, host cell proteins

Kurzfassung:

Der Einfluss der Geschwindigkeit auf die Prozessleistung wurde für zwei partikelförmige Protein A Affinitätsgele untersucht. MabSelect PrismA von GE Healthcare ist ein Gel basierend Hochfluss-Agarose und Toyopearl AF-rProtein A HC-650F besitzt ein Polymethacrylat-Rückgrat. Beide Gele besitzen rekombinante Protein A Liganden, die gegenüber alkalischer Regeneration resistent sind. Der Einfluss der Geschwindigkeit auf die dynamische Bindungskapazität war erwartet und ist auch in der Literatur gut dokumentiert. In dieser Arbeit wurden verschiedene Geschwindigkeiten für Wasch- und Elutionsschritte in mit Fokus auf den Gehalt an Wirtszellprotein und die Aggregation eines monoklonalen Antikörpers (mAb) getestet. Dieser Einfluss war jedoch für die Toyopearl-Gele eher gering und für MabSelect PrismA vernachlässigbar. Die Antikörperaggregation konnte unter keinen Verfahrensbedingungen detektiert werden, selbst nicht für sehr raue Elutionsbedingungen. Für Toyopearl wurde ein höherer Gehalt an Wirtszellprotein in den Eluaten bestimmt, wenn die Säule bei niedriger Proteinsättigung oder höheren Geschwindigkeiten betrieben wurde. Dieses Ergebnis ist primär auf Interaktionen von Wirtszellproteinen mit dem Gel Rückgrat zurückzuführen. Ein Waschschritt mit einer Isopropanol und Harnstoff enthaltenden Pufferlösung führte zu sehr niedrigen Verunreinigungsmesswerten für das Toyopearl Gel, während sie für MabSelect PrismA nur mäßig wirksam war. Der Einfluss der Geschwindigkeit auf diese Reinigung war jedoch sehr gering. Insgesamt legen die Ergebnisse dieser Studie nahe, dass der Betrieb von Protein A Affinitätsmedien bei hoher Geschwindigkeit die Abtrennung von Wirtszellproteinen nicht beeinflusst. Wobei die Zusammensetzung des Waschpuffers eine größere Rolle spielt. Diese Ergebnisse sind wichtig im Hinblick auf die neue Protein A Affinitätsmembran, die derzeit bei Sartorius entwickelt wird.

Stichworte:

mAb, Protein A , Einfluss der Geschwindigkeit, Wirtszellproteine

Dictionary of Abbreviations:

As – Asymmetry

AID - Activation-induced (Cytidine) deaminase

C – Concentration

C_F – Concentration of feed

C_H – Constant of heavy chain

C_L – Constant of light chain

C_{ref} – Reference concentration

CCS – Cell culture supernatant

CDR – complementary determining region

CHO – Chinese hamster ovary

D_e - Effective pore diffusion coefficient

$\check{D}_e$ – Apparent diffusion coefficient

D_p – Pore diffusion coefficient

D_s – Solid diffusion coefficient

D_H – Diversity for heavy chain

Da – Dalton

DBC – Dynamic binding capacity

d_p – Particle diameter

EBC – Equilibrium binding capacity

ELISA – Enzyme-linked immunosorbent assay

Fab – Fragment antigen binding

Fc – Fragment crystallisable

Fv – Fragment of antibody containing only the paired V_H and V_L domains

HETP – height equivalent to a theoretical plate

HCP – Host cell protein

HPLC – High pressure liquid chromatography

h – Reduced HETP

Igs – Immunoglobulins

J_H – Joining for heavy chain

K – Equilibrium constant

K_p – steric hindrance parameter

k_f – Film mass transfer coefficient

L – Column length

mAb – monoclonal antibody

N – Plate number

PBS – Phosphate buffer solution

q_m – Static binding capacity

R – Separation factor

r_m – gyration radius of molecule

r_p – Particle radius

r_{pore} - Radius of pore

SEC – Size exclusion chromatography

TdT – Terminal deoxynucleotidyl transferase

t_R – residence time

u – Superficial mobile phase velocity

V_L – Variable of light chain

V_H – Variable of heavy chain

v – Interstitial velocity of mobile phase

W_b – distance between baseline intercepts of the tangents to the inflection point of the peak

W_h – width at half peak height

ε – Bed porosity

ε_b – Total bed porosity

ε_p – Particle porosity

λ_m – ratio of gyration radius of pore and radius of pore

μ_1 –mean residence time

σ – Variance

τ – Tortuosity factor

$\tau 1$ – Dimensionless time

Table of contents

1 Introduction

1.1 Today's antibody market

In the past five years the monoclonal antibody (mAb) market has doubled its size. Furthermore, there is a trend to new bispecific antibodies, conjugated molecules and focusing onto fully human mAbs. Therefore, in 2017 two-thirds of the new approved mAbs were fully human. A lot of the mAbs currently on the market can target multiple diseases, but most of them have at least one cancer target, which is rendered by the total of 15 mAbs targeting oncology diseases. All mAbs on the market belong to one of the IgG subclass and the majority are IgG1 with 79%. Moreover, mammalian cell lines are the favoured expression system, applied in 61 out of 66 commercial bioprocesses due to their ability to glycosylate.
In December 2017 the mAb market exceeded a value 0f US$98 billion in sales, and showed a growth between 7.2% and 18.3% as shown in Figure 1. In the future, the market will be positively influenced by faster approval speed within the pipelines, but will be negatively influenced by the approval of biosimilars and drug conjugates. The most manufactures are located in the US or in Europe whereat seven companies hold 87% of the total market. It is indicated, that the mAb market will reach sales from US$ 130-200 billion until 2022 [6].

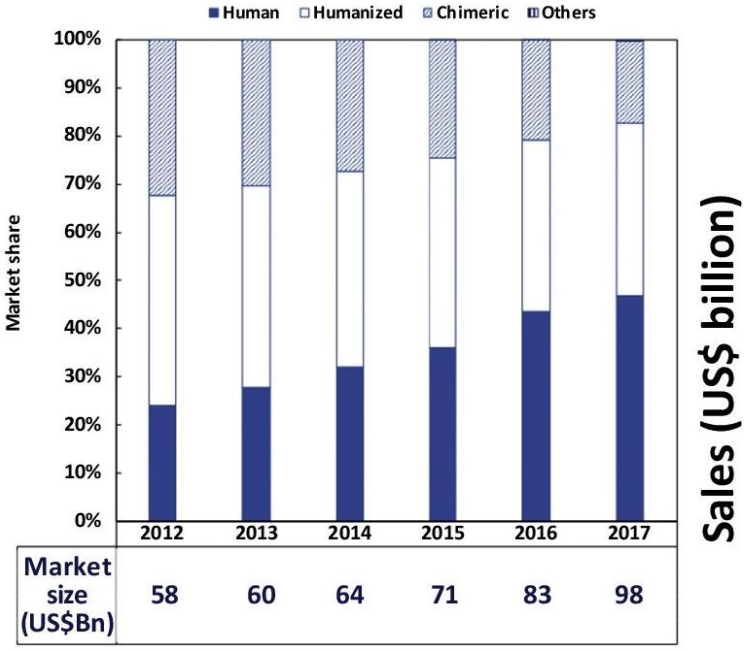

Figure 1: Growth of today's antibody market since 2012 until 2017, distinguishing between human, humanized and chimeric mAbs [6]

Commercial issues for the use of mAbs are the high treatment costs of administration. It has also been shown that in cancer treatment the use of antibodies were not always curative and could in some cases only extend the median survival compared to classic chemotherapy. Moreover, in some cases the administration of antibodies can lead to side effects, like infusion reactions or cardiac symptoms. [7]

1.2 Antibodies and their function, structure and diversity

1.2.1 General principle of antibody generation and function

Antibodies are soluble proteins that are generated by plasma cells and B cells and respond to non-self-antigens. Antibodies or immunoglobulins (Igs) can bind a single antigen very specific and furthermore can provide effector functions. Therefore, antibodies control the spread of infections by the recognition of pathogens and their products.
B cells are specialized lymphocytes, which present preformed antibodies on their surface. For the production of specific antibodies, the B cells have to first bind an antigen with the antibodies presented at their surface. This interaction induces the phagocytosis of the pathogen and further leads to the killing of the pathogen. The B cell then produce a great variety of pathogen-derived antigens that are presented to the antigen-specific T helper cells.

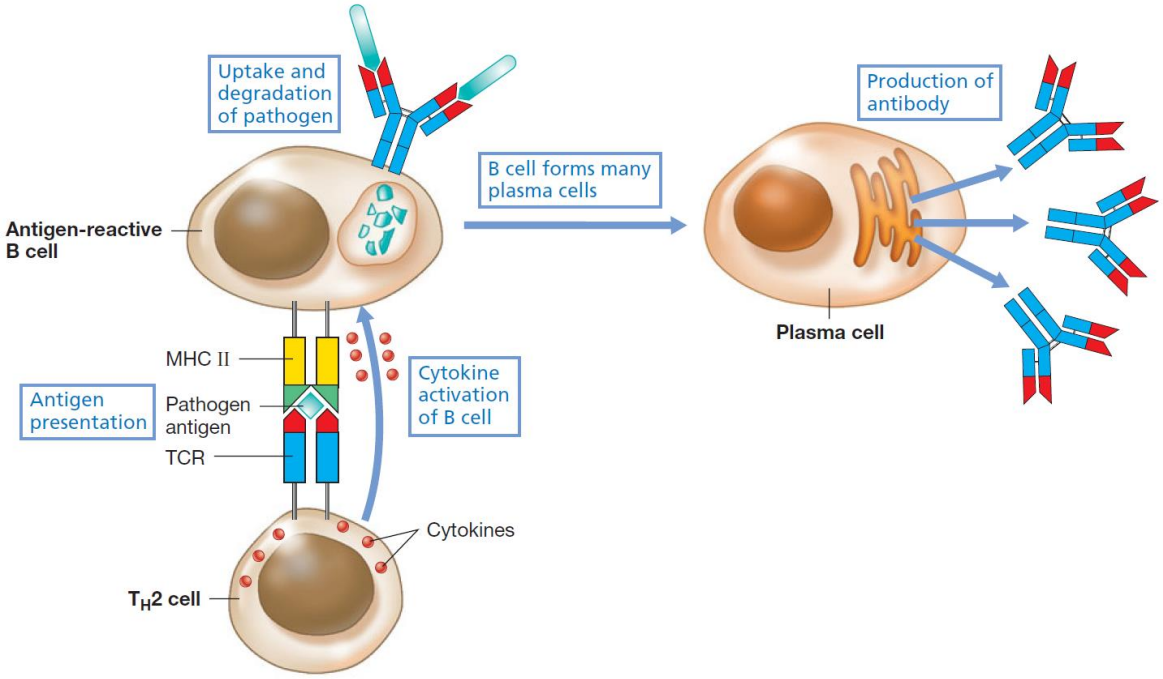

Figure 2: Mechanism of generation of antibodies in humans [1]

These helper cells do not interact directly with the pathogens but support antigen-reactive B cells by producing cytokines that respond by growing, dividing and establishing clones of the original antigen-reactive B cell. Furthermore, this B cell differentiate into antibody producing plasma cells. This specific adaptive response can induce the immune memory and a second adaptive response which is characterized through a more rapid development of higher quantities of antibodies[1].

1.2.2 Chemical structure and variability of antibodies

Antibodies are large and complex proteins that can accomplish a broad range of functions and possess different functional domains which are responsible for their various functions. In general, all human antibodies consist of two identical heavy chains of 50-75 kDa that are paired with a pair of identical light chains of 25 kDa giving the antibody its characteristic Y-shaped structure.

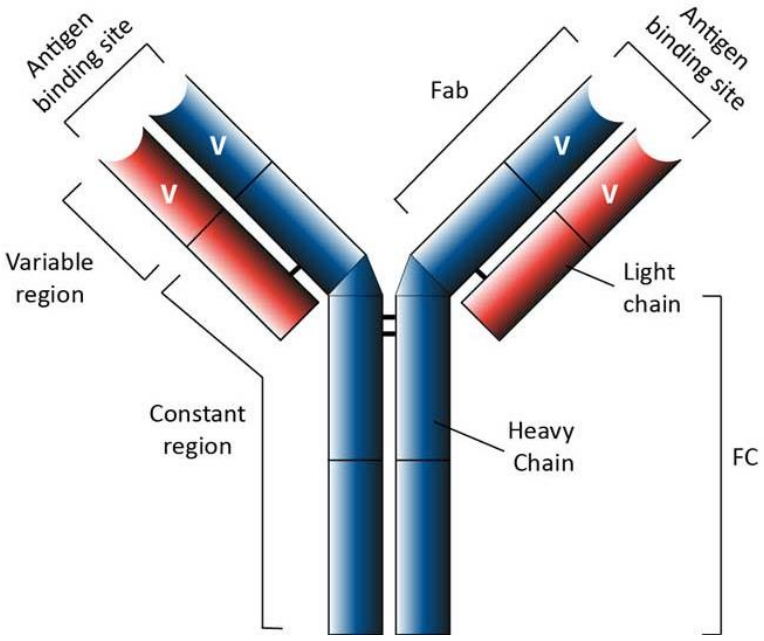

Figure 3: Schematic description of a monoclonal antibody, comprising out of a light and heavy chain and further showing the active regions of the antibody consisting out of an antigen binding site and a constant region for effector functions [4]

Furthermore, there are five major classes of antibodies; IgA, IgD, IgE, IgG and IgM which are defined through the sequence of the heavy chain which are α, δ, ε, γ and μ. Whereas the light chains are either κ or λ isoforms for all classes[3].

The different antibody classes comprise various functions and therefore have diverse localizations. The primary immune response is characterized through a high production of IgM and further on larger amounts of IgG, which are both found in the blood. IgA is also found in the blood, but mainly in the mucous membrane secretions. IgE is localized on mast cells and plays an important role in parasite immunity and allergies. IgD is found on the surface of B cells. One can distinguished between two major regions the Fc ("fragment, crystallisable") and the Fab ("fragment, antigen binding) region which are both consist of ß-pleated sheets [3].

1.2.2.1 Fc

The Fc consist of a CH_2 domain which is fused to a CH_3 domain, whereas the two CH_3 domains bind each other tightly compared to the CH_2 which does not have a direct protein-protein interaction. Furthermore, within the two CH_2 domains there is a glycosylation site on an asparagine residue. Krapp et al 2003 and Matsumiya et al 2007 observed hydrogen bonding between the two carbohydrate chains [8, 9].

1.2.2.2 Fab

In general, the Fab fragment comprises of four domains: the heavy chain variable domain (V_H) connected to the heavy constant domain 1 (CH_1), and the light chain variable domain (V_L) which is connected to the constant domain of the light chain (C_L). The Fab fragment was originally generated by cleavage of IgG with papain that generates two individual Fab fragments. Furthermore, a cleavage with pepsin leads to a $F(ab')_2$ which is connected via disulphide bridges. The complementary determining regions (CDR) are created by packing of the variable domains, V_L and V_H, and is responsible for antigen combining/binding. Moreover, proteolytic cleavage of the Fab fragment leads to the Fv fragment which only contains V_L and V_H regions and only comprises the CDR. Fv showed to be very unstable and prone to aggregation[3].

1.2.2.3 Hinge region

The hinge connects the Fc with the Fab regions and provides a rotational flexibility and an independent orientation of the Fabs. The hinge is only found on IgG, IgD and IgA heavy chains. In principle, the hinge can be divided into three parts, the upper hinge, the core hinge and the lower hinge. The upper hinge gives flexibility and rotational ability to the Fab, whereas the core hinge connects the heavy chains through disulphide bridges. Motion of the Fc part is provided by the lower hinge and contributes to the binding of the Fc to the Fc neonatal receptor[3].

1.2.3 Antigen variability of Antibodies

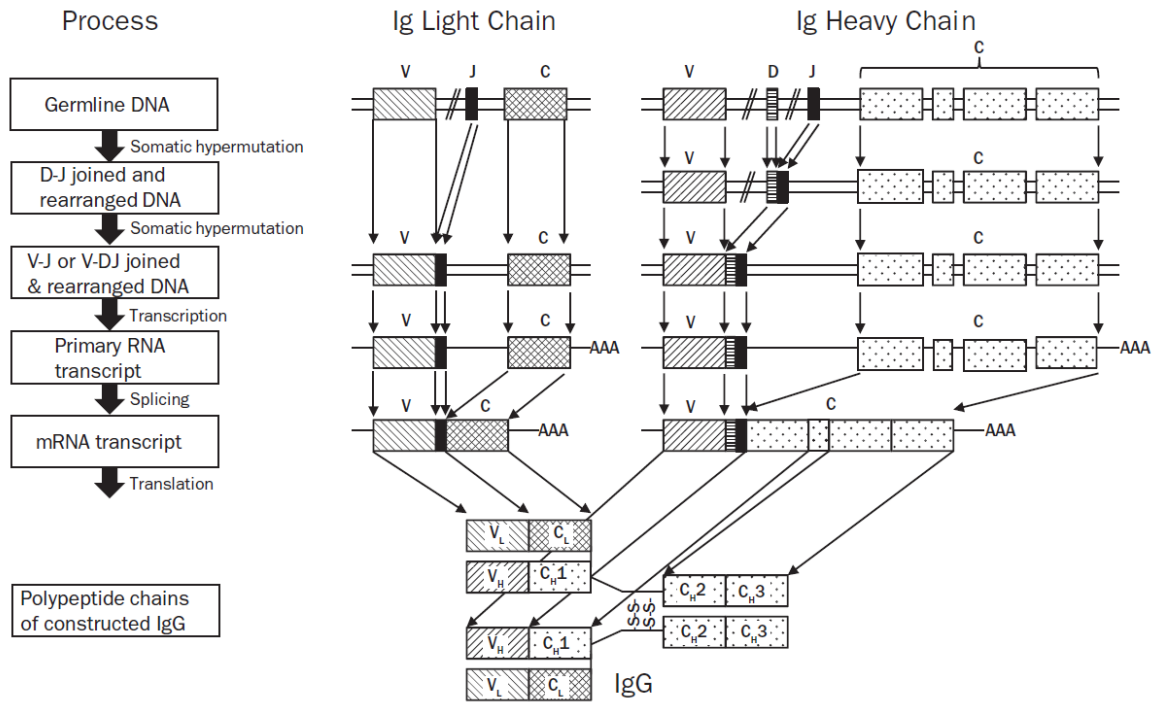

Figure 4: Description of generating antibody diversity of light and heavy chains [3]

In human, the antibodies consist of a heavy and a light chain that are encoded by 14 genes and three gene families, the kappa, the lambda and a family of nine heavy chain genes. The antibody classes (IgG, IgA, IgM, IgD and IgE) and the subclasses (IgG_1, IgG_2, IgG_3, IgG_4, IgA_1, IgA_2) are defined by nine different heavy chains. Isotypes are generated by combining the particular heavy chain class or subclass with one of the light chains kappa or lambda. Allotypes are allelic variants within the constant regions and exist for six heavy chain loci and the kappa locus. Idiotypes comprise an exceptional combination of V_H and V_L chains that creates the combining site.

The generation of human antibody diversity is a complex process, which involves multiple actions of creating diversity. In general, there are two repertoires, the pre-immune repertoire where antibodies are generated against foreign targets, and the post-immune repertoire were antibodies against foreign antigens are selected and matured.

Basically, the diversity is generated by combining V_H, D_H, J_H chains with V_H and V_L chains to construct a complete antibody. The combinatorics is based on joining 39 functional V_H chains with 27 functional D genes and six J_H chains. Furthermore, there are four possibilities to generate more diversity. First, the translation of the D genes can take part in one of three reading frames in both directions, generating another six variants. Second, the formation of a hairpin within the rearrangement process can lead to addition or deletion of nucleotides. Third, deletions or additions of nucleotides can occur during the VDJ joining process. Furthermore, within the joining of the VDJ junctions, the activity of the terminal

deoxynucleotidyl transferase (TdT) can lead to further nucleotide addition or replacement[3]. This makes up the CDR-H3 part in the functional V-region and therefore comprises a great variation of 10^7 variations of CDR-H3 and a change in length of few to 25 amino acids. Concluding, the potential of the diversity of all antibody in the pre-immune repertoire is $>10^{16}$ and that these immunoglobulins have a relatively low affinity to antigens [10, 11].
The second immune response is triggered via the affinity maturation process, where antibodies that show high affinity to the antigen, are further selected through the creation of new diversity. In general, there are two major processes which are responsible for generating diversity, the somatic hyper mutation and the class-switch recombination. The somatic hyper mutation is characterized through a mutational hotspot defined by the amino acid sequence RGYW which represent the complement of the substrate site for Activation-Induced (Cytidine) Deaminase (AID). Therefore, this site is targeted for AID-mediated mutation, in which single strand DNA is deaminated to form dU/dG mismatches, DNA glycosylase removes the mismatched dU, which further leads to a mutation in the synthesis strand. In the second mechanism, the target is a base pair mismatching between the template and the newly synthesized DNA which results in an nucleotide change [12].

1.2.4 CHO as expression system for mAbs

The Chinese hamster ovary (CHO) cell line is one of the most popular cell lines for the production of mAbs and Fc fusion proteins. CHO is favoured because of its long safety record, very good growth and productivity in serum-free medium. In general, mammalian cell lines are preferred among others because of their ability to glycosylate. A lot of transgene transfection and amplification methods were tested, among which the DHFR-deficient CHO cell lines are the most favoured[3, 13].
The history of CHO is going back to 1957 and cell lines have undergone three main stages of improvement and innovation. First approach was to improve recombinant protein titre, which was contributed through media optimization, genetic engineering (selection processes, expression vectors…), the design of bioreactors and their process control. In the second strategy, the focus was on improving the per-cell yield by cell engineering, which was done by metabolic engineering, knock-in strategies and particularly use new methods like ZFNs, TALENs and CRISPR/Cas9. The last stage in the development of CHO cell lines was the characterisation and the engineering of protein secretion systems. Various omics techniques have been used to study productive clones and revealed diverse up-and down-regulating reactions and connections [14].

1.3 Protein A, an ancient defence mechanism and magnificent tool for mAb purification

Staphylococcal protein A is a 42 kDa surface protein that is located on the cell wall of the gram-positive bacterium Staphylococcus aureus and has a high affinity to IgG. The origin of protein A indicates that this protein is a native defence mechanism against the immune system.[15] Due to this specific binding it is a magnificent example for an affinity ligand. Protein A is constructed out of three regions, whereas the S region is the signal sequence and the IgG binding domain is composed out of five homologous domains E, D, A, B and C. Moreover, the region XM is responsible for the cell-wall attachment.[16-18] The structure of the five domains of Protein A is built up from an anti-parallel three alpha-helical bundle that is stabilized by the hydrophobic core. The Fc-part of an antibody is independently bound by each of the five domains and shows a high affinity to IgG_1, IgG_2 and IgG_4 but only low affinity to IgG_3.[15, 19]

Concerning stability of Protein A, lot of effort was taken to enhance protein stability especially for cleaning and regeneration procedures. Therefore, enhanced stability to chemical cleavage was introduced in B's domain via site directed mutagenesis leading to the Z domain (Z4), which nowadays is a synthetic analogue of the native B domain. Recent protein A resins for example Mab Select SuRe from *GE Healthcare* have a designed ligand comprising four repeats of the Z domain to be alkaline resistant[19, 20]. Moreover, an exchange or prolonging in the loop region between helix one and two lead to a higher elution pH. For the tolerance of high pHs, several site specific mutagenesis were contributed. Especially exchange of asparagine residues was evaluated, due to deamination and backbone cleavage in alkaline environment and an exchange with Threonine lead to higher stability.[19] Furthermore, the generation of histidine-substituted variants of protein A lead to a shift of the elution pH from 4.2 to 5.6 due to electrostatic repulsion under acidic condition. Additionally the thermal stability was enhanced by this substitution.[21] On the other hand, it was reported that an exchange of histidine to serine in the Z domain also leads to higher elution pH and could be further increased by exchanging Asparagine against Alanine.[20] This is favourable in industrial processes because elution at low pH can lead to aggregation and further to side effects in patients.

1.4 Host cell proteins

Therapeutic proteins are produced in genetically engineered prokaryotic or eukaryotic cells, but these cells also produce their own proteins. These endogenous proteins, which are derived from the host cell, are called host cell proteins (HCP) and belong to the process-related impurities[22]. HCP can elicit immune response and furthermore influence the product quality by triggering aggregation or fragmentation [23-25]. Therefore HCP content should be reduced as much as possible, whereas EMA states that the individual acceptance criteria should be set as appropriate oriented on preclinical and clinical studies and manufacturing consistency lots[26]. A commonly accepted level of HCP is in the range of 1-100 ppm. The most used method for quantification is the ELISA assay whereas there are also alternatives like SELDI-TOF, FT-MIR, 2D-DIGE and 2D-LC/MS[22].

HCPs are regarded as a critical factor and are very difficult to predict, as the HCP profile can vary with cell type, cell state, media formulation, amino acid sequence and with cultivation type/mode and time [27]. Furthermore, many HCPs are associated with the therapeutic protein itself, for example mAbs, which can even show differences in HCP content within various mAbs [28]. Concluding, there are many various interactions possible which can take place between mAb and HCPs, like hydrophobic interaction, electrostatic repulsion, hydrogen bonds Van der Waal's force, ionic interaction and the presence of immunoglobulin-like domains. This leads to the strong intention to reduce such interactions in Protein A chromatography through introduction of diverse washing procedures with urea, propylene glycol, isopropanol, arginine, sodium chloride and sodium caprylate [27]. It was also reported that the amount of regeneration cycles of agarose based resins show an increase of HCP associated on the resin and thereby influencing the DBC but not the HCP content in the eluates [29]. Previous studies have shown that there are interactions between the resin backbone and the HCP which are crucial for higher HCP content in eluates. Furthermore, the matrix composition of the resin is defining which species of HCP can bind to the column itself due to the resulting interactions taking place. This lead to the fact that for the various resins a specific washing procedure could be introduced [30-32].

1.5 Chromatography

1.5.1 Chromatographic principle

Chromatography is a separation technique comprising of a stationary phase and a mobile phase. The stationary phase interacts with the solute and the mobile phase transports the solute through the solid phase. There are various interactions taking place in chromatography but in general, the mixture of components must be partitioned differentially between the mobile and the stationary phase to generate a separation. Usually, the mixture of components is supplied at one end of the fixed bed and individual components are separated over time and length of the column. Therefore, the collection of components is carried out at the end of the bed due to different residence times.

In general, one can distinguish between three modes of operation, elution chromatography, frontal chromatography and displacement development. Elution chromatography is based on the interaction between the feed and the stationary phase and the mobile phase which flows through the column and has less affinity to the stationary phase. The mobile phase flows through the column and the feed components migrating in the direction of flow according to their affinity to the stationary phase. Furthermore, there are isocratic elution and gradient elution that differ in a way, that in isocratic elution the mobile phase stays constant and in gradient elution the mobile phase changes over time and volume. In the frontal analyses the feed is dissolved in an appropriate mobile phase and is fed to the column continuously. Within the column the mixtures of the different components are strongly absorbed which leads to a formation of bands whereat the weakest adsorbed components

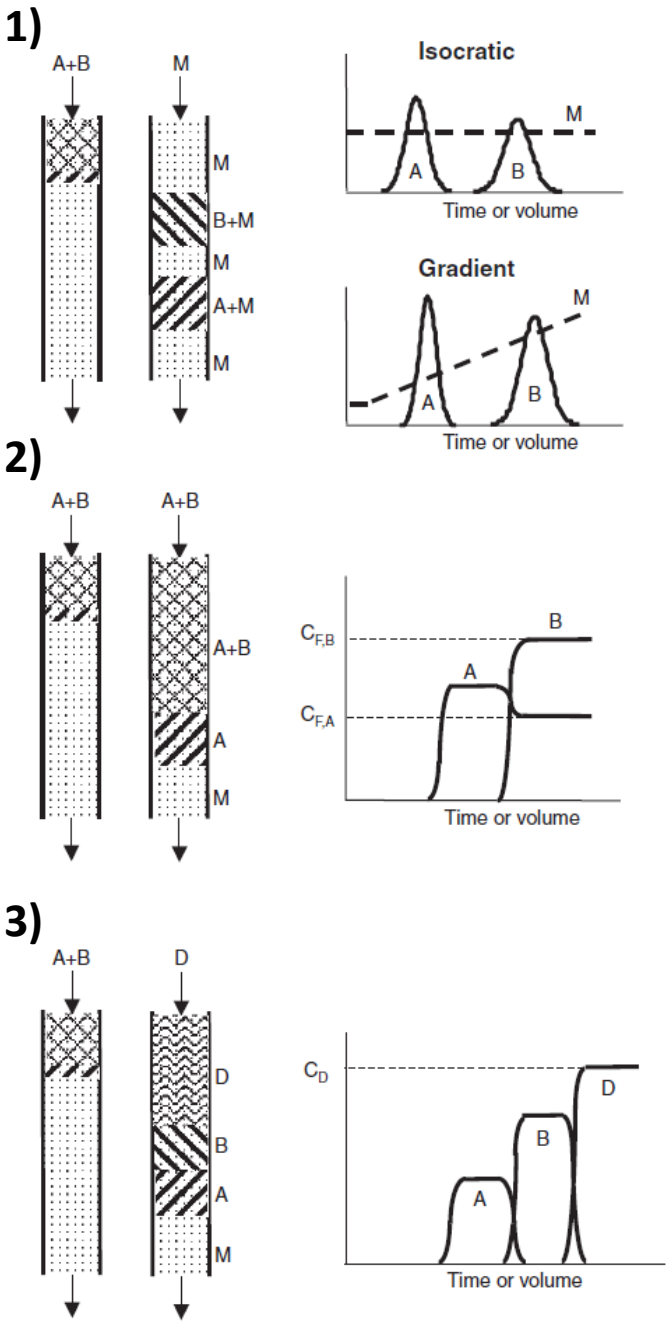

Figure 5: Schematic description of the three major chromatography realizations; 1) elution chromatography, 2) frontal chromatography and 3) displacement chromatography [2]

move fastest. Usually this technique is used to partition impurities that are strongly interacting with the stationary phase. Therefore, the product can be collected at the outlet until column saturation is reached. In displacement chromatography, the column is also loaded with a feed and mobile phase mixture but only for a specific time. Afterwards the mobile phase is changed to a composition that has stronger interaction than any component of the feed. Therefore, the new mobile phase displaces the bound components leading to a cascade of readsorption downstream. In the optimal situation, all components will travel through the column at the same velocity leading to a fractionation of components.[2]

1.5.2 Characteristic parameters and definitions in chromatography

Chromatography is usually performed in packed beds that are filled with spherical porous particles which are responsible for the adsorption process. The chromatographic system is generally coupled to a monitoring system equipped with detectors like UV, pH and conductivity, adapted to the process. In general, buffers and samples are fed to the top of the column and components are separated due to their interaction with the stationary phase. Concerning protein chromatography, mainly water-based buffers are used, as organic solvents can denaturate proteins. In this thesis the major focus was laid on protein chromatography [2].
Chromatographic media are generally composed of spherical matrices. It can be distinguished between polysaccharides (agarose, dextran, cellulose…), synthetic organic polymers (polymethacrylate, polystyrene, polyacrylamide…) and inorganic materials (hydroxyapatite, silica).

Equation 1: Total bed porosity

$$\varepsilon_b = \varepsilon + (1 - \varepsilon)\varepsilon_p$$

The particle morphology is characterised by the particle porosity ε_p, representing the space filled with liquid in ratio to the total volume of the particle. The particle porosity is very dependent on the matrix material and can range from 0.5 for synthetic polymers to 0.98 for polysaccharide-based matrices. The external void fraction ε is the fraction of interstitial liquid between the packed particles. Combining these two factors, the total bed porosity (ε_b) can be written as shown in Equation 1 [33].
Stationary phases can be generated through crosslinking and grafting, providing high chemical stability and adopted particle and pore size for the intended use. In general, every chromatographic medium exhibits a size distribution of particles and pores [2, 33]. For preparative protein A chromatography the particle sizes reach from 45 µm to 90 µm, whereas for protein A chromatography the ligand stability has an important role [34].

Equation 2: Langmuir isotherm

$$q = \frac{q_m K C}{1 + KC}$$

The adsorption of proteins is characterised by the adsorption isotherm, which defines a model of the equilibrium relationship between the concentration of protein in the fluid phase (C) and the concentration of protein on the stationary phase (q). The Langmuir isotherm is the most often used and is described in Equation 2. Where q_m is the maximum binding capacity and K is the equilibrium constant.

Equation 3: Separation factor

$$R = \frac{1}{1 + KC_{ref}}$$

The dimensionless separation factor is expressed in Equation 3, in which C_{ref} is a reference concentration of the feed or the initial values encountered in the process. This factor indicates the nonlinearity of the isotherm, whereas R=1 means linear, R<1 corresponds to favourable and R=0 to rectangular isotherm which represents irreversible adsorbtion. Furthermore R>1 indicates that the isotherm is unfavourable. In Protein A chromatography it is assumed to work with a rectangular adsorption isotherms indicating very strong adsorption [33].

1.5.3 Mass transfer in chromatography

The external mass transfer between the external surface of the particle and the fluid phase is the first step in the adsorption process. The driving force is the concentration difference across the boundary layer and is affected by the liquid film which depends on the hydrodynamic conditions outside of the particle. Therefore, the film mass transfer coefficient k_f depends on the particle size, fluid viscosity and fluid velocity. In principle k_f is concentration dependent but this is neglectalbe as long as the viscosity is not strongly affected. In preparative protein chromatography k_f can be neglected, except for very low protein concentrations and/or when intraparticle mass transfer is enhanced, for example by solid diffusion [2, 33].
The intraparticle transport into macro porous media can be expressed using a pore diffusion coefficient D_p which is in general lower than the unhindered diffusion in a cylindrical pore because of the tortuous shape and the varying pore diameters defined by the media. Both effects can be compensated by introduction of a correction factor, the tortuosity factor (τ), whereas τ=4 as proven to be a good estimation for chromatographic media in bioseparations. Furthermore, diffusion is also affected by steric hindrance between the molecule and the pore walls leading to size exclusion effects and viscous drag forces[33].

Equation 4: Steric hindrance parameter for λ_m<0.2

$$K_p = \left(1 + \frac{9}{8}\lambda_m ln\lambda_m - 1.539\lambda_m\right) \quad for\ \lambda_m < 0.2$$

Equation 5: Steric hindrance parameter for λ_m>0.2

$$K_p = 0.865(1-\lambda_m)^2\left(1 - 2.1044\lambda_m + 2.089{\lambda_m}^3 - 0.984{\lambda_m}^5\right)\ for\ \lambda_m > 0.2$$

Equation 6: Ratio of gyration radius of molecule to pore size

$$\lambda_m = \frac{r_m}{r_{pore}}$$

Therefore, a steric hindrance parameter K_p was introduced that can be calculated using Equation 4 and

Equation 5. Whereas λ_m expresses the ratio of the radius of gyration of the molecule (r_m) to the radius of the pore (r_{pore})[2, 33].
The effective pore diffusion coefficient can be expressed as according to Equation 7, whereas diffusion coefficients for proteins are typically between 5 x 10^{-8} and 8 x 10^{-7} cm²/s [2].

Equation 7: Effective pore diffusion coefficient

$$D_e = \varepsilon_p D_p = K_p \frac{\varepsilon_p D}{\tau}$$

In pore diffusion, proteins can diffuse into the pores, where they can be attached and detached many times, but in favourable isotherms the proteins can bind nearly perpetual. In contrast to pore diffusion, in solid diffusion transport the adsorbed state is taking place without detachment occurring. Targets for this kind of transport can be on the pore surface or surface extenders. In general, solid diffusion is driven by a concentration gradient in the adsorbed phase, and is described through the effective solid-phase diffusion coefficient (D_s). The value of solid diffusion coefficient is usually 100 times lower for proteins, as for pore diffusion. However, solid diffusion is, in contrast to pore diffusion, concentration dependent thus that very low protein concentrations increase the apparent diffusivity ($\check{D}_e$)[33].

Equation 8: Model diffusional mass transfer for spherical particles

$$\varepsilon_p \frac{\partial c}{\partial t} + \frac{\partial q}{\partial t} = \frac{1}{r^2}\frac{\partial}{\partial r}\left[r^2\left(\varepsilon_p D_p \frac{\partial c}{\partial r} + D_s \frac{\partial q}{\partial r}\right)\right]$$

Boundary conditions:

$$t = 0 : c = 0, q = 0$$
$$r = 0 : \frac{\partial c}{\partial r} = 0$$
$$r = r_p : \varepsilon_p D_p \frac{\partial c}{\partial r} + D_s \frac{\partial q}{\partial r} = k_f (C - c)$$

In Equation 8 a model for diffusional mass transfer for spherical particles including pore and solid diffusion is given. In which c and C corresponds to the concentration in the pore fluid and in the external fluid and r_p refers to the particle radius, representing the left term of the equation represents the pore fluid concentration and the accumulation in the particle, whereas the right side expresses the diffusion into a pore of a spherical particle[33].
Mass transfer is mainly dominated by the factors of media structure, protein properties and adsorption conditions. Generally, pore diffusion is the major mass transfer contributor in macro porous gels with wide pores and at high binding strength. Solid diffusion is the major contributor if composite media are used. The overall/apparent diffusivity can be written as:

Equation 9: Apparent diffusivity distinguishing between solid and pore diffusion

$$\check{D}_e = D_e + D_s \frac{q_m}{C}$$

1.5.4 Column performance and packing quality

Column packing is generally performed according to the suppliers' manual, but usually packing buffers contain around 0.15 M of NaCl and 10 – 20% ethanol for weakening electrostatic interacting. Evaluating the packing quality of columns is a very crucial point and is usually performed with a NaCl pulse or acetone pulse under nonbinding buffer conditions. The obtained peaks are evaluated by their statistical moments.

Equation 10: Definition of plate number

$$N = \frac{{\mu_1}^2}{\sigma^2}$$

Equation 11: Height equivalent to a theoretical plate

$$HETP = \frac{L}{N}$$

Calculating the plate number (N) and the resulting height equivalent to a theoretical plate (HETP) represents a measure of the peak dispersion. Equation 10 and Equation 11 show

correlation of these variables, whereas μ_1 refers to the mean residence time, σ^2 refers to the variance and L to the column length.

Equation 12: Calculation of plate number (1)

$$N = 5.54(\frac{t_R}{W_h})^2$$

Equation 13: Calculation of plate number (2)

$$N = 16(\frac{t_R}{W_b})^2$$

These evaluations are susceptible to signal noise and base line drifts, therefore approximations can be used, which are shown in Equation 12 and Equation 13. Whereby t_R is the time at maximum attitude, W_h refers to the peak width at half peak height and W_b refers to the distance between the baseline intercepts of the tangents to the inflection point of the peak. Furthermore, HETP is a characteristic parameter for measuring the influence of the dispersive factors on chromatographic performance in relation to the component of interest. This also includes the defined operation conditions such as chromatography material, column format and flow rate. The van Deemter equation is given in Equation 14 and expresses the relationship of HETP to the flow rate.

Equation 14: Van Deemter equation

$$H = A + \frac{B}{u} + Cu$$

Whereas A refers to the Eddy dispersion which are caused by flow nonuniformities and mixing effects and B refers to the longitudinal molecular diffusion. The parameter C refers to mass transfer effects.

Combination of chromatographic parameters like fluid velocity, diffusivity and particle diameter leads to dimensionless quantities like Reynolds number and Schmidt number which are given in Equation 15 and Equation 16.

Equation 15: Reynolds number

$$Re = \frac{ud_P}{v}$$

Equation 16: Schmidt number

$$Sc = \frac{v}{D}$$

Whereas in Equation 15 and Equation 16, the d_p is the particle diameter, D the molecular diffusion coefficient, u the superficial velocity and *v* the kinematic viscosity.

Equation 17: Reduced HETP and the corresponding Van Deemter equation

$$h = \frac{HETP}{d_p} = a + \frac{b}{ReSc} + cReSc$$

Furthermore, HETP can be expressed as reduced HETP (h) which is given in Equation 17. For protein chromatography, HETP can be determined under non-binding conditions and the HETP is controlled by mass transfer referring to pore and solid diffusion[33].

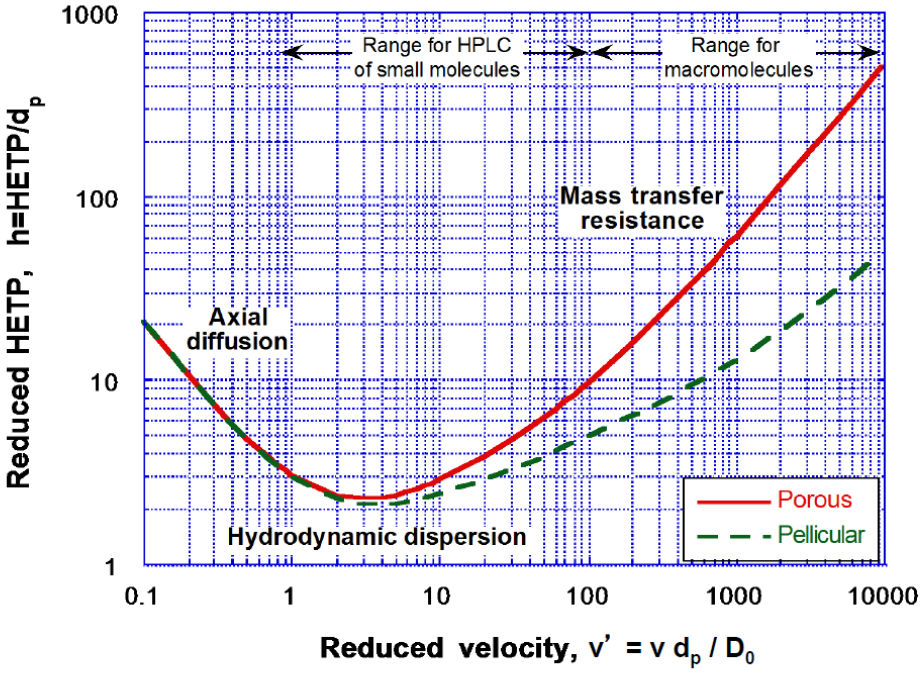

v = mobile phase velocity, d_p = particle diameter, D_0 = diffusivity in mobile phase

Figure 6: Relation of reduced HETP with reduced velocity revealing dominant mass transfer parameters for chromatographic applications [2]

An additional parameter for the evaluation of the packing quality is the asymmetry which is defined in Equation 18.

Equation 18: Asymmetry

$$A_s = \frac{b}{a}$$

Whereas *a* refers to the area on the left side of the peak tip and *b* to the right. In general values for asymmetry should range from 0.8 to 1.5[2].

1.5.5 Breakthrough curves

In preparative protein chromatography, the most important parameter is the dynamic binding capacity (DBC). For the determination of the DBC usually a series of experiments are performed in which chromatographic media are loaded with sample at different loading velocities. Furthermore, the load of protein is chosen to achieve saturation, where unbound protein starts to leave the column. The shape of the obtained breakthrough curves is usually characterised by various factors including adsorption isotherm, particle size and effective diffusivity. Generally, the DBC is defined referring to a certain amount of breakthrough, usually 5 or 10%[2].

Equation 19: Expression of dimensionless time

$$\tau_1 = \left(\frac{ut}{L} - \varepsilon\right)\frac{C_0}{(1-\varepsilon)q_0}$$

Equation 20: Expression of transfer units using column and matrix parameters

$$N = \frac{15(1-\varepsilon)D_e L}{u{r_p}^2}$$

Furthermore, the generated breakthrough curves can be used to determine the effective pore diffusion coefficient (D_e) by applying a model given in Equation 19 and Equation 20, whereas τ_1 is the dimensionless time and N the transfer units. In general, the protein solution concentration of the load is rather small compared to the adsorption capacity, which makes it possible to express the DBC as a fraction of the static binding capacity. Rearrangement to τ_1 leads to the Equation 21[33].

Equation 21: Simplified expression of the dimensionless time for C/C_0=0.1

$$\tau_1 = \frac{DBC}{(1-\varepsilon)q_0} \quad for \frac{C}{C_0} = 0.1$$

For a DBC at 10% breakthrough the constant pattern solution for pore diffusion can be expressed as given in Equation 22.

Equation 22: Constant pattern solution for the dimensionless time at C/C_0=0.1

$$\tau_1 = 1 - \frac{1.03}{N}$$

The effective pore diffusion coefficient can be determined by plotting the obtained capacities at 10% breakthrough divided by the static binding capacity versus the residence time. The constant pattern solution is only valid for $N\tau_1 \geq 2.5$, but for short residence times there is an empirical approximation, the general solution, which is given in Equation 23[33].

Equation 23: General solution for the dimensionless time

$$\tau_1 = 0.364 * N - 0.0612 * N^2 + 0.00423N^3$$

Fitting experimentally generated data points to these equations makes it possible to determine the effective pore diffusion coefficient for the case that pore diffusion is the dominating factor[33].

Equation 24: Residence time

$$\tau = \frac{L}{u}$$

Rearranging Equation 20 gives the estimation for the D_e, as the residence time (τ) can be expressed as shown in Equation 24. For more detail see section 3.5 below. Furthermore, it is possible to estimate the diffusion coefficient with another approach, referring to the model of the shrinking core. Assuming that the isotherm is rectangular, which is often the chase for protein chromatography and also using the constant pattern, which can be expressed as shown in Equation 25. The term lighted in grey can be neglected and for X=0.1 the model can be simplified to give Equation 22[2].

Equation 25: Constant pattern solution for pore diffusion and film diffusion

$$N_{pore}(1-\tau_1) = +\frac{15}{2} ln\left[1+(1-X)^{\frac{1}{3}}+(1-X)^{\frac{2}{3}}\right] - \frac{15}{\sqrt{3}} tan^{-1}\left[\frac{2}{\sqrt{3}}(1-X)^{\frac{1}{3}}+\frac{1}{\sqrt{3}}\right] - \frac{n_{pore}}{n_{film}}[ln(X)+1] + \frac{5\pi}{2\sqrt{3}} - \frac{5}{2}$$

Boundary conditions:

$$X = \frac{C}{C_F},\ N_{pore} = \frac{15\phi D_e}{{r_p}^2}\frac{L}{v}, N_{film} = \frac{3\phi k_f}{r_p}\frac{L}{v}$$

$$\phi = \frac{(1-\varepsilon)}{\varepsilon}$$

1.5.6 Affinity chromatography forward to protein A chromatography

In general, affinity chromatography is based on the specific binding of a target molecule and a complementary ligand. This method can achieve high operational yields and reduce undesired contaminants because of its high specificity of its binding. Therefore, this method can be operated in a one-step process by simply disrupting the highly specific interaction by the right choice of eluent[35]. This elution can be achieved through addition of denaturation agents, change of pH, ionic strength or polarity, or through adding of competing analogues [36]. In principle, in affinity chromatography the specific ligand is immobilized onto a solid matrix, which can be agarose, glass, methacrylate, or other matrices. Usually the chromatographic procedure is based on five steps; equilibration of the column, load of the sample, wash out of unbound components, elution with appropriate buffer and regeneration of the column which is summarized in Figure 7.

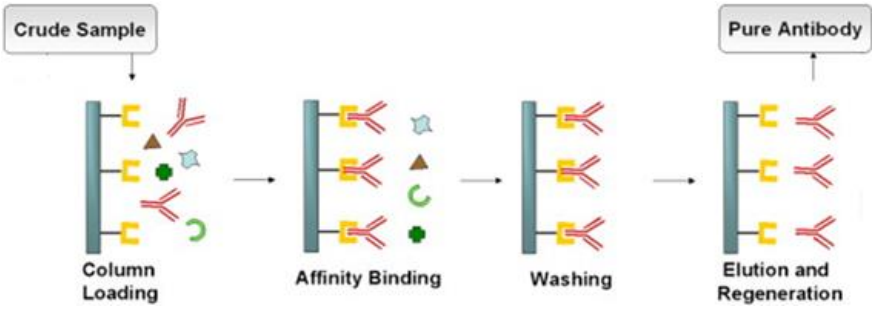

Figure 7: Characteristic steps in affinity chromatography [35]

Protein A chromatography is an excellent example of an affinity chromatography used for the purification of mAbs where it is usually used a capture step[19]. The highly specific binding of the Fc region of the antibody can achieve impurity removal of over 95% within a single step. However, protein A ligands tend to be very expensive therefore an appropriate regeneration method with sodium hydroxide is state of the art. This cleaning procedures can have a high impact on ligand stability and longevity therefore great efforts have been made to improve alkaline stability [19, 20, 37]. Furthermore, classic column chromatography tends to have high back pressures and even clogging and fouling can occur which results in a reduction of operating velocities[35]. Additionally, studies have shown that especially the DBC of different protein A resins is effected by the matrix composition, whereas agarose based resins showed a higher DBC at low velocities and Polystyrenedivinylbenzene showed better performance at higher velocities implying that the residence time plays a very important role. Furthermore, particle size strongly contributes to the DBC because larger particles require longer residence times for efficient mass transfer. It has also been shown that for large molecules like mAbs the pore diffusion is the main factor that contributes to the overall mass transfer which is usually higher for small particles but these can lead to high backpressures[38]. Improvement and investigation of chromatography matrices lead to high performance resins, suitable for a good manufactural processes. These new resins like Mab Select SuRe or ProSep-vA Ultra have a high

binding capacity and good mass transfer properties, which can be achieved by a high ligand density and big pores. Furthermore, determination of the effective pore diffusion coefficient of common protein A resins indicate that the D_e is inversely proportional to the feed concentration[39].

1.5.7 Membrane Chromatography

The reprocessing of large-scale bioprocesses has led to an increase in the demands of downstream processing such as manufacturing costs, high through put and (semi)-continuous processes. Drawbacks of classical protein A chromatography, like ligand stability and low capacities have been overcome, but new high producing cell cultures and single use technologies require fast and capable downstream processes. Common drawbacks of column chromatography based on spherical resins are high backpressures, high costs, slow operating velocities and slow mass transfers[40]. The usage of membrane chromatography could overcome these drawbacks especially because the mass transfer is not driven by diffusion but by convection. In general, one can distinguish between a flat sheet, a hollow fibre or a radial flow operation mode which is shown in Figure 8. In the flat sheet membranes, the feed is usually applied normal to the membrane surface, whereas in the hollow fibre the feed flows parallel to the membrane surface. In the radial flow membrane, the feed is applied similar to the hollow fibre but it is flowing through more like in a flat sheet. Although the flow is not distributed consistently, this operation mode is one of the most favoured in the industry[5].

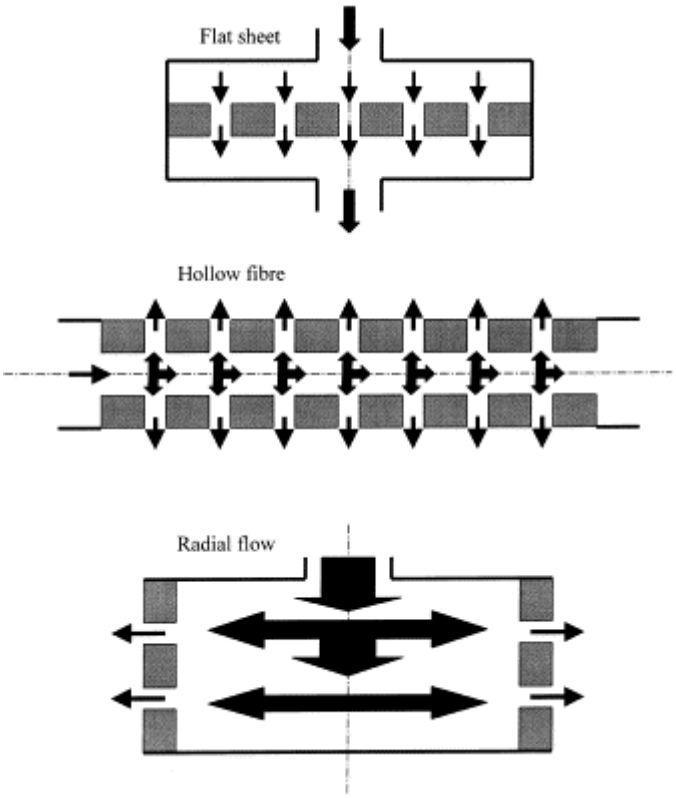

Figure 8: Principle of the three major membrane chromatography variants; flat sheet, hollow fibre and radial flow [5]

Focusing on protein A chromatography the flat sheet operation mode is probably more favoured due to more predictable flow distribution and simplicity and it can also overcome the drawbacks of the column chromatography[41]. Furthermore, membrane chromatography has shown to be an effective method to purify mAbs from cell culture supernatant, with equal HCP content as observed in a column chromatography[40].

In principle there are some challenges observed in membrane chromatography which are the inlet flow distribution, the membrane pore distribution, the membrane thickness and the low binding capacity[5]. Concerning the flow distribution, laterally-fed membrane techniques have been reported that overcome the problem of low resolution through this lateral feed method, which leads to a strongly increased resolution[42, 43]. Pore size distribution and uneven membrane thickness are factors that could be overcome by manufacturing improvement and investigation, and the choice of the right support material. Additionally it has been shown that these issues could be overcome by the use of membrane stacks[44]. Furthermore, the binding capacity could be improved by ligand editing, improving specific surface area or by coating the pores with a porous polymer [5].
Due to these characteristics affinity based membrane chromatography would be a fast and economic tool for the purification of mAbs form a cell culture supernatant[41]. Furthermore, using membrane chromatography has even shown to have high separation potential because it was possible to purify charge variants of IgG1 [45].

1.6 Aim of the study

The initial goal of this study was a comparison of the performance of a new Protein A membrane, which is currently under development at Sartorius, with conventional Protein A resins based on spherical beads. As the development of the new Protein A membrane is not yet finished, it was decided to perform a study with only conventional resins focusing on effects related to velocity. Besides velocity of the loading step, also velocity effects during washing and elution steps were studied in detail because these topics are not well covered in the scientific literature on Protein A affinity chromatography. Furthermore, understanding of these effects is useful for later comparison and designing operating conditions once the new membrane is available. For this purpose two high performing Protein A resins with very high binding capacity, Toyopearl AF-rProtein A HC-650F from Tosoh Bioscience and Mab Select PrimsA from GE Healthcare were used. The culture supernatant containing a monoclonal antibody was provided by Sartorius, all experimental work was carried out at the Department of Biotechnology, BOKU Vienna.

2 Materials and Methods

2.1 Reagents and equipment used for the experiments

Buffer reagents were purchased from Merck (Darmstadt, Germany) and Sigma-Aldrich (St. Louis, MO). Acetic acid which was purchased from *VWR* (Radnor, PA) and TMB peroxidase EIA Substrate Kit from *Bio-Rad* (Hercules, CA).
Toyopearl AF-rProtein A HC-650F was obtained from *Tosoh Bioscience* (Tokyo) and Mab Select PrimsA from *GE Healthcare* (Uppsala, Sweden). The chromatographic media were packed into 2 mL Tricorn^{TM} 5 columns (*GE Healthcare,* Uppsala, Sweden). All chromatographic experiments were carried out on an ÄKTA^{TM} Explorer 100 system (*GE Healthcare,* Uppsala, Sweden). The used supernatant contained an IgG1 monoclonal antibody expressed in Chinese hamster ovary (CHO) cells which was kindly provided by *Sartorius* (Göttingen, Germany).

2.2 Experimental set up

The CHO cell culture supernatant was thawed and sterile filtered prior to every experiment. The UV signal was monitored at a wavelength of 300 nm because the signal at 280 nm exceeded the detector limit due to high protein concentration. Fraction collection was started when the UV signal exceeded 50 mAU and stopped when the signal was lower than 100 mAU. In general, one-millilitre fractions were collected, which were immediately neutralized with 1 M TRIS/HCl buffer pH 8, to achieve a neutral pH of the fraction to avoid aggregate formation and precipitation. Principally, the equilibration was conducted with 1xPBS and the elution was carried out with acetic acid pH 3. Furthermore, the columns were regenerated with 0.25 M sodium hydroxide for Toyopearl and 0.5 M sodium hydroxide for PrismA. All buffers were degassed in an ultrasonic bath for 15 minutes prior to use.

2.3 Analytical set up

Protein determination was conducted by measuring the absorbance at 280 nm using a Photometer Cary 60 UV-VIS from *Agilent Technologies* and a one-centimetre quartz cuvette (Santa Clara, CA). Additionally, the protein concentration was determined by an analytical protein A chromatography using the POROS A20 from *Applied Biosystems* (Foster City, CA) and the HPLC system 1220 infinity LC, from *Agilent Technologies* detecting with DAD detector also at 280 nm. Furthermore, the aggregate formation was detected by analytical size exclusion chromatography (SEC) using Superdex 200 increase column from *GE Healthcare* (Uppsala, Sweden) and a HPLC system alliance e2956 from *waters* (Milford, MA). The host cell protein (HCP) content was measured by an ELISA test method from *Cygnus Technologies Inc.* (Southport, NC)

2.4 Chemicals and reagents

Table 1: Chemicals and reagents used for conducted experiments

Chemicals and reagents:	
name	**supplier**
Monoclonal antibody - CHO supernatant	***Sartorius***
Bovine serum albumin	***Sigma***
TMB Peroxidase EIA Substrate Kit	***Bio-Rad***
Tween 20 Polysorbate	***Sigma***
Sodium chloride	***Merck***
Potassium cholride	***Merck***
0.25 M sulphoric acid	***Merck***
Disodium phosphate dihydrate	***Merck***
Monopotassium phosphate	***Merck***
Sodium hydrogen carbonate	***Merck***
Sodium carbonate	***Merck***
Natrium hydroxid	***Merck***
Hydrochloric acid	***Merck***
Urea	***Sigma***
Citric acid	***Sigma***
Isopropanol	***Sigma***
Glycine	***Merck***
acetic acid	***VWR***
TRIS	***Merck***
Ethanol	***VWR***

2.5 Analytical devices and apparatus

Table 2: Analytical devices and apparatus used for analysing

Description	Name	Supplier
Prep. LC	**ÄKTA™ Explorer 100**	***GE Healthcare***
Anal. HPLC/LC	**1220 infinity LC**	***Agilent Technologies***
Anal. HPLC/LC	**alliance e2695**	***waters***
Photometer	**Cary 60 UV-VIS**	***Agilent Technologies***
Plate reader	**infinite M2000 Pro**	***Tecan***
Balance	**NewClassic MF, MS3002S**	***Mettler Toledo***
pH electrode	**SevenEasy**	***Mettler Toledo***
Multi-channel pipette	**E4 XLS**	**Rainin**

Table 3: Used resins and analytical columns

Description	Name	Supplier
Protein A resin	**Mab Select PrismA**	***GE Healthcare***
Protein A resin	**Toyopearl AF-rProtein A HC-650F**	***Tosoh Bioscience***
Analytic Protein A column	**POROS A20**	***Applied Biosystem***
Analytic SEC column	**Superdex 200 increase, 10/300**	***GE Healthcare***
HCP-ELISA	**CHO-HCP***	***Cygnus Technologies***

- See detailed description

2.6 ÄKTAexplorer 100 System

The used chromatographic system for all experiments was an *ÄKTA Explorer 100* system from *GE Healthcare*. The ÄKTAexplorer 100 is a liquid chromatography system, which offers a completely automated system. The separation unit is composed of three major parts, which are localised on the left side of the platform. The first one is the pump system which consist out of the pump P-900 and is a binary high performance gradient pump accomplishing up to 100 mL/min and a pressure up to 10 MPa. Furthermore, the system comprises a UV-900 multi-wavelength unit, which can simultaneously monitor three wavelengths in the range of 190 nm-700 nm. The third part consists of a pH/C-900 monitor, which combines online conductivity, and pH monitoring. The entire system can be fully automated using the Software UNICORN which was also used for this study (Version: UNICORN 5.11, 2006).

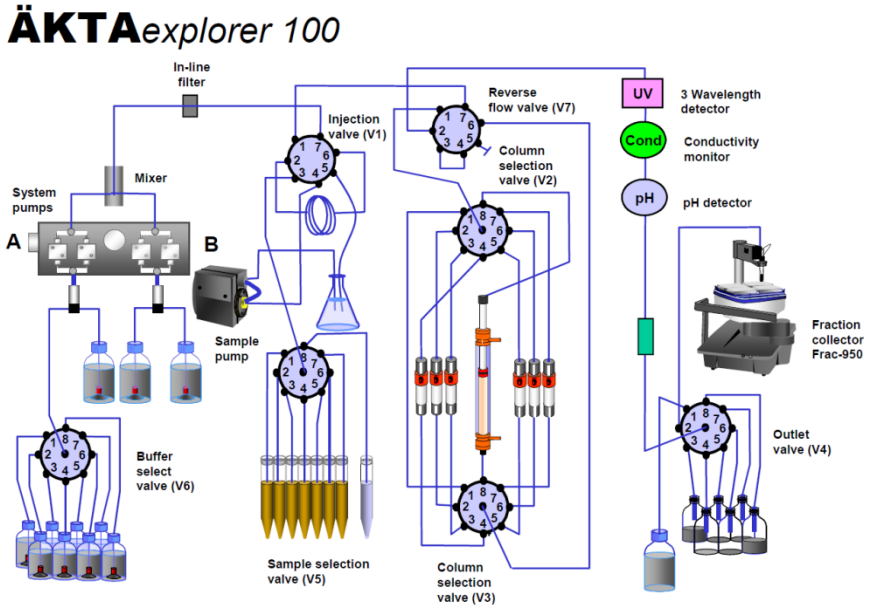

Figure 9: Scheme of ÄKTAexplorer 100 system

2.7 Experimental assembly for mAb purification

In general, all experiments were conducted using the ÄKTAexplorer 100 system monitoring the UV signal at 300 nm, the pH and the conductivity. The wavelength of 300 nm was chosen instead of 280 nm because of the signal intensity at 280 nm reached the maximum. Within the experiments the UV detector was automatically calibrated and the pH electrode was calibrated before every set of runs. The elution peaks were collected in one-millilitre fractions which, were immediately neutralized to a pH value of approximately 7 with a stock solution of 1 M TRIS/HCl buffer pH: 8.0. Therefore, 300 µl of buffer were added to each millilitre of fraction. This was done to prevent the concentrated antibody from precipitation. The peak collection was adjusted to start collecting when exceeding a UV signal of 50 mAU and stopping the fractionation when the signal was lower than 100 mAU, as the UV signal did not completely go back to zero.

The equilibration buffer for all experiments was 1xPBS which was also used to wash out the unbound sample after loading. After every elution step there was a regeneration step which was performed with sodium hydroxide. Mab Select PrismA was regenerated with 0.5 M sodium hydroxide and Toyopearl AF-rProtein A HC-650F with 0.25 M sodium hydroxide. Before every regeneration step the column was re-equilibrated with 1xPBS to avoid high backpressures. The entire ÄKTA system and both columns were stored in 20% ethanol when not in use. Channels, connections and vessels been in contact with cell culture supernatant were additionally rinsed with 0.1 M sodium hydroxide. All used buffers were degassed in an ultrasonic bath for 15 minutes to reduce noise of the UV detector. The supernatant provided from Sartorius was thawed, sterile filtered (0.22 µm) and conditioned to room temperature before every experiment.

2.7.1 Determination of Dynamic binding capacity (DBC) and buffer screening

In the first section, the focus laid on the determination of the dynamic binding capacity (DBC) of both resins. Therefore, sufficient amount of sample was loaded to achieve a breakthrough. Furthermore, this experiment was combined with a screening of the elution buffers. The detailed experimental set-up is shown in Table 4. Furthermore, all collected fractions were analysed for protein content, aggregate formation and HCP content. Additionally, another run for each resin was conducted at 200 cm/h which was overloaded to reach a full breakthrough and a fully saturated gel. The obtained breakthrough curve was fitted by a pore diffusion model which was used to estimate the effective diffusion coefficient (D_e) and maximum capacity (q_m). With these parameters r predicting breakthrough curves at different loading velocities were predicted. Furthermore, the flow through was collected and analysed to set up a closed mass balance. For the breakthrough experiments, the mAb load was kept constant and only the loading velocity was varied ranging from 75 cm/h to 400 cm/h. Additionally, this experiment was combined with an elution buffers screening in which some common elution buffers were tested.

Table 4: Experimental set up for DBC

	Column:	Load (mL)	Velocity (cm/h)	Elution buffer	Elution velocity (cm/h)
1)	Mab Select PrismA	60.0	75	100 mM HAc, pH: 2.9	150
2)	Mab Select PrismA	60.0	100	25 mM HAc, pH: 3.2	150
3)	Mab Select PrismA	60.0	150	100 mM citrate buffer, pH: 3.0	150
4)	Mab Select PrismA	60.0	300	100 mM citrate buffer, pH: 3.2	150
5)	Mab Select PrismA	60.0	400	100 mM glycine buffer, pH: 3.0	150
1)	Toyopearl AF-rProtein A HC-650F	60.0	75	100 mM HAc, pH: 2.9	150
2)	Toyopearl AF-rProtein A HC-650F	60.0	100	25 mM HAc, pH: 3.2	150
3)	Toyopearl AF-rProtein A HC-650F	60.0	150	100 mM citrate buffer, pH: 3.0	150
4)	Toyopearl AF-rProtein A HC-650F	60.0	300	100 mM citrate buffer, pH: 3.2	150
5)	Toyopearl AF-rProtein A HC-650F	60.0	400	100 mM glycine buffer, pH: 3.0	150

2.7.2 Variation of mAb loading and loading Velocity

In the next section, it was investigated how the gel saturation and loading velocity affects HCP content and aggregate formation. Therefore, the experiments were conducted to achieve three levels of gel saturation, in which both resins were loaded to approximately 90% of possible loading without breakthrough, at three different loading velocities, 100, 200 and 400 cm/h, respectively. Variation of the loading amount was achieved by keeping the loading velocity constant at 100 cm/h and applying three different amount of mAb, referring to the amounts loaded in previous experiments to obtain three levels of loading amount. All other parameters were kept constant to achieve comparability. The precise experimental set-up is shown in Table 5 below.

Table 5: Experimental set up of variation of load and loading velocity

	Column	Saturation (mg/mL)	Load (mL)	Velocity (cm/h)	Elution buffer
1)	Mab Select PrismA	10	7.7	400	56 mM HAc pH 3.0
2)	Mab Select PrismA	40	30.7	200	56 mM HAc pH 3.0
3)	Mab Select PrismA	60	46.0	100	56 mM HAc pH 3.0
4)	Mab Select PrismA	10	7.7	100	56 mM HAc pH 3.0
5)	Mab Select PrismA	40	30.7	100	56 mM HAc pH 3.0
1)	Toyopearl AF-rProtein A HC-650F	15	9.8	400	56 mM HAc pH 3.0
2)	Toyopearl AF-rProtein A HC-650F	50	32.6	200	56 mM HAc pH 3.0
3)	Toyopearl AF-rProtein A HC-650F	65	42.4	100	56 mM HAc pH 3.0
4)	Toyopearl AF-rProtein A HC-650F	15	9.8	100	56 mM HAc pH 3.0
5)	Toyopearl AF-rProtein A HC-650F	50	32.6	100	56 mM HAc pH 3.0

2.7.3 Variation of elution velocity

In this task, the effect of the elution velocity on the HCP content and the aggregate formation was investigated. Therefore, the standard purification procedure was kept constant and only the elution velocity was varied at 100, 200 and 400 cm/h. The exact experimental assembly is shown in Table 6.

Table 6: Experimental set up of variation of elution velocities

	Column	Saturation (mg/mL)	Load (mL)	Elution buffer	Elution velocity (cm/h)
1)	Mab Select PrismA	40	30.7	56 mM HAc pH 3.0	100
2)	Mab Select PrismA	40	30.7	56 mM HAc pH 3.0	200
3)	Mab Select PrismA	40	30.7	56 mM HAc pH 3.0	400
1)	Toyopearl AF-rProtein A HC-650F	50	37.3	56 mM HAc pH 3.0	100
2)	Toyopearl AF-rProtein A HC-650F	50	37.3	56 mM HAc pH 3.0	200
3)	Toyopearl AF-rProtein A HC-650F	50	37.3	56 mM HAc pH 3.0	400

2.7.4 Introduction of a pre-elution step and variation of velocity

In the final step, an additional phase was introduced that is targeting the elution of impurities and HCP under slightly acidic conditions which is described by Shukla et al 2008[32] and is also recommended from the resin supplier. This pre-elution phase is located prior the common elution step. Therefore, small-scale experiments were carried out to determine a suitable pH value for this pre-elution step. Adopting the method from Shukla et al 2008 [32], a 50 mM citrate buffer was selected as pre-elution buffer. Furthermore, the experimental set up was designed to test three different pre-elution velocities (100, 200 and 400 cm/h) and their influence on recovery, HCP content and aggregate formation. The experiments were suited to only obtain a weak signal of protein (280 nm) during the pre-elution, and therefore should not affect the recovery.

Table 7: Experimental set up of the variation of pre-elution velocities

	Column	Saturation (mg/mL)	Pre-elution buffer	pre-elution vel./ CV (cm/h)
1)	Mab Select PrismA	40	50 mM citrate buffer, pH 5.0	100/3
2)	Mab Select PrismA	40	50 mM citrate buffer, pH 5.0	200/3
3)	Mab Select PrismA	40	50 mM citrate buffer, pH 5.0	400/3
1)	Toyopearl AF-rProtein A HC-650F	50	50 mM citrate buffer, pH 5.0	100/3
2)	Toyopearl AF-rProtein A HC-650F	50	50 mM citrate buffer, pH 4.8	200/3
3)	Toyopearl AF-rProtein A HC-650F	50	50 mM citrate buffer, pH 4.8	400/3

2.7.5 Implementation of an intermediate wash to reduce HCP

In the last section, the objective was to further improve HCP clarification by introducing an intermediate wash using a TRIS/HCl buffer at pH 9 with 10% Isopropanol and 1 M urea [32]. This step was incorporated between the PBS wash and before the start of the pre-elution. The influence of the intermediate wash on the HCP content was investigated by varying the washing velocity and the wash intensity, time of contact respectively. Therefore, the velocities 100 and 400 cm/h tested for 4 and 8 column volume washes.

Table 8: Experimental set up of introduction of an intermediate wash

	column	Saturation (mg/mL)	intermediate wash buffer	intermediate Wash velocity/CV (cm/h)
1)	**Mab Select PrismA**	**40**	**TRIS pH 9, 10% Isopropanol, 1M Urea**	**400/4**
2)	**Mab Select PrismA**	**40**	**TRIS pH 9, 10% Isopropanol, 1M Urea**	**400/8**
3)	**Mab Select PrismA**	**40**	**TRIS pH 9, 10% Isopropanol, 1M Urea**	**100/4**
4)	**Mab Select PrismA**	**40**	**TRIS pH 9, 10% Isopropanol, 1M Urea**	**100//8**
1)	**Toyopearl AF-rProtein A HC-650F**	**50**	**TRIS pH 9, 10% Isopropanol, 1M Urea**	**400/4**
2)	**Toyopearl AF-rProtein A HC-650F**	**50**	**TRIS pH 9, 10% Isopropanol, 1M Urea**	**400/8**
3)	**Toyopearl AF-rProtein A HC-650F**	**50**	**TRIS pH 9, 10% Isopropanol, 1M Urea**	**100/4**
4)	**Toyopearl AF-rProtein A HC-650F**	**50**	**TRIS pH 9, 10% Isopropanol, 1M Urea**	**100/8**

2.8 Protein determination with photometer

For the investigation of the protein content, the Photometer *Cary 60 UV-VIS* form *Agilent Technologies* was used and all measurements were carried out in quartz cuvettes with a path length of 1 cm. The determination of the protein amount of the eluted fractions was done by measuring the absorbance at 280 nm. Therefore, appropriate dilutions of the factions were done in 1xPBS to be in the linear range of the photometer. All measurements were carried out in duplicates and the blank signal (only 1xPBS without sample) was subtracted from the measured values. Finally, Equation 26 was used to calculate the protein concentration of the diluted sample and furthermore calculating the entire amount of protein in the sample as it is shown below.

Equation 26: Determination of protein amount using photometric methods

$$Protein\ amount\ (mg) = \frac{A_{280}}{\varepsilon(1.4)} * DF * V_{elution}$$

2.9 Protein determination with analytical Protein A

Furthermore, a second method for the determination of the protein content of the eluted fractions and the supernatant was used. For that purpose an HPLC *1220 infinity LC* from *Agilent Technologies* and an analytical protein A column, *POROS A20* from *Applied Biosystem* were used. The operating mode was a step elution, whereas the equilibration was performed with 1xPBS and the elution was done with a 12 mM HCl as shown in Table 9. The signal was detected with a DAD at 280 nm. The system was calibrated with a purified mAb from Sartorius, which was determined with UV_{280nm} in triplicates assuming an extinction coefficient of ε = 1.4. The calibration ranged from 0.05 mg/mL to 2.5 mg/mL and the samples were diluted in 1xPBS to be in the calibration range.

Table 9: Method for step elution of analytical protein A chromatography

	1xPBS	HCl 12 mM
min	A%	B%
0	100	0
1.5	100	0
1.51	0	100
2.5	0	100
2.51	100	0
5	100	0

2.10 Analytic SEC for determination of aggregate formation

All eluted fractions were analysed with a SEC to detect aggregate formation of the antibody. The used system was the HPLC alliance e2695 from *waters* and the column was a *Superdex 200 increase, 10/300* from *GE healthcare*. The operation mode was an isocratic elution with 50 minutes per sample at a flow of 0.5 mL/min and 1xPBS as a running buffer. The detection was carried out at 280 nm and 214 nm.

2.11 CHO-HCP ELISA

For the determination of the HCP content all eluted fractions were analysed with the CHO HCP ELISA (*Cygnus*) assay. The obtained results were converted to part per million (ppm) using the previously determined protein content. In Table 10 all required buffers, materials and antibodies needed for the performance of the CHO HCP ELISA assay are listed.

Table 10: Composition and materials of all used buffers necessary for carrying out the ELISA assay

Buffers:	**Composition:**
Coating buffer	0.2 M carbonate buffer pH: 9.3-9.5
Blocking buffer	3% BSA in 1xPBS
Sample buffer	1% BSA, 0.05% Tween 20 in 1xPBS
Washing buffer	0.05% Tween 20 in 1xPBS
10% Tween	10% Tween in 1xPBS
10xPBS	17.8 g/L Na_2HPO_4*$2H_2O$, 2.4 g/L KH_2PO_4, 2.0 g/L KCL, 80 g/L NaCL in H_2O

Materials:	**Supplier:**
NUNC 96F for dilution	NUNC
NUNC MaxiSorp Immuno plate	NUNC

CHO Antibodies and standard:	**supplier:**
Capture Antibody: Anti-CHO HCP affinity purified	Cygnus/3G-0016-AF
Detection Antibody: Anti-CHO HCP:HRP conjugate concentrate, 3 G	Cygnus/F551C
Standard: CHO HCP Antigen concentrate (22 µg/mL)	Cygnus/F553H

In this ELISA assay, the detection plates were self-coated which was done with the Anti-CHO HCP antibody that was diluted 1:800 in coating buffer. Furthermore, 100 µl of the diluted antibody were pipetted in each vial and the plate was sealed to prevent drying out. The plate was incubated for 2 hours at 37°C under moderate shaking (300 – 350 rpm). After the incubation time the solution was discarded and the plate was washed with the washing buffer by pipetting in 300 µl into each vial. Further on, this solution was discarded as well and the entire procedure was repeated twice (3x plate washing). After washing the plates, 300 µl of the blocking buffer was transferred into each vial, sealed and incubated overnight at 4°C at moderate shaking (300 – 350 rpm). Before the application of the samples, they had to be diluted on a dilution plate (96 well plate) in sample buffer. Every plate contained at least one blank and two standards, which were treated equally. The standard solution was diluted 1:200 in sample buffer, which gave a concentration of 110 ng/mL and lead to a calibration curve ranging from 110 ng/mL to 0.86 ng/mL. For the dilution, 170 µl of sample buffer were pipetted in each vial of the plate, except the first row. In the first row, the samples were applied by pipetting in 340 µl of sample. Then, 170 µl from the first row were pipetted into the second row (from A to B). The solution was mixed by pipetting 8 – 10 times up and down. This procedure was repeated throughout the entire plate. Afterwards, the overnight-incubated plate was washed according to the washing procedure and then 100 µl of the dilution plate of each vial were transferred to the detection plate, sealed and incubated for 1 hour at 37°C under moderate shaking. After the sample application, the plate was washed again and then assembled with the secondary antibody that was diluted 1:2000 in sample buffer. Therefore, 100 µl of this solution were transferred to each vial of the plate and incubated at 37°C for 1 hour under moderate shaking. Before the application of the staining solution, the plate was washed according to the washing procedure. The staining solution was prepared by mixing nine parts of the TMB solution A of the TMB Peroxidase EIA Substrate Kit with one part of the TMB solution B (hydrogen peroxide). After washing, there were transferred 100 µl of the staining solution into each vial, sealed and incubated for 30 minutes at room temperature. Finally, 50 µl of 0.25 M sulphuric acid were added to each vial. The absorbance was measured at 450 nm together with the subtracted reference wavelength at 630 nm using the *Tecan* plate reader. The data evaluation was done using MS Excel. The obtained standard curve was fitted into a quadratic trend line ($y=ax^2+bx+c$) and gave a R^2 of 0.999 and a bias of maximum 15%. The samples were evaluated by calculating the mean with at least three values.

3 Results and Discussion

3.1 General

In the first work package the focus was on determination of the dynamic binding capacity (DBC) and an elution buffer screening. Furthermore, an additional run was performed to obtain a complete breakthrough curve for estimation of the effective diffusion coefficient. In the next work package it was investigated how the gel saturation and the loading velocity affects HCP content and aggregate formation. In work package three, the effect of the elution velocity was investigated. Implementation of a pre-elution step was also conducted. In the last work package an additional washing step with varying wash velocity and amount of washing buffer was introduced. All obtained eluates were analysed with respect to recovery, aggregate formation and HCP content.

3.2 Column packing

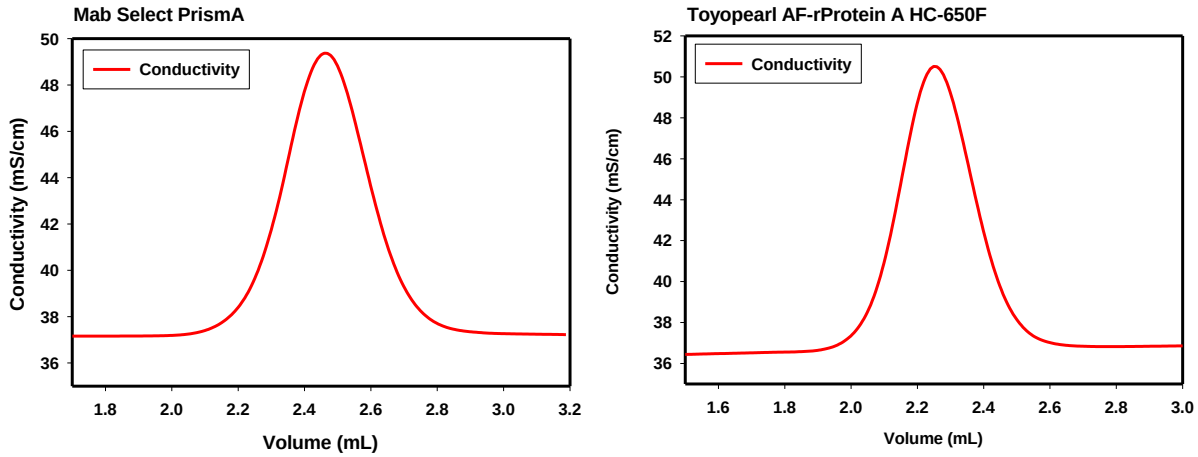

Figure 10: Equilibration of protein A columns with low salt buffers and subsequent salt pulse with 1.2 M NaCl for evaluation of packing quality

The column packing was carried out according to the manual instructions provided by the manufacturer. All columns were packed on an ÄKTA^{TM} Explorer 100. After equilibration with 0.4 M NaCl, columns were pulsed with 1.2 M NaCl at a velocity of 100 cm/h. The obtained conductivity profiles were evaluated using the programs UNICORN and Peakfit. UNICORN uses numerical peak integration whereas Peakfit analysis is based on fitting an exponentially modified Gauss (EMG) function to the peak profiles. Plate number (N), height equivalent to a theoretical plate (HETP) and reduced HETP (h) were calculated from the first and second peak moment, and column height and particle diameter, respectively. Calculated values are summarized in Table 11. Generally, two columns were packed for both resins, whereas the second one was always used as a back-up column. For Toyopearl AF-rProtein A HC-650F 3

columns had to be packed because this resin tended to create high overpressure, which lead to clogging of the column. Overall, values for *h* were in a range of 4-8. In general, for simple affinity chromatography using a step elution, the reduced HETP is of minor importance as in lab scale the columns are used up to a reduced HETP of >8 [34]. This acceptance range is based on the fact that extra-column effects occurring in lab scale columns lead to significant extra peak broadening in small scale.

Table 11: Obtained parameters for the evaluation of packing quality

	PrismA (1)		Toyopearl (1)		Toyopearl (2)		Toyopearl (3)	
	length (=10.9 cm)		length (=10.6 cm)		length (=9.3 cm)		length (=9.3 cm)	
	UNICORN	Peakfit	UNICORN	Peakfit	UNICORN	Peakfit	UNICORN	Peakfit
Plates (N)	429.6	396.9	453.4	418.1	274.2	255.25	367.6	379.1
Asymmetry	1.06	1.08	1.16	1.13	1.03	1.06	1.05	1.04
HETP (cm)	0.02538	0.02747	0.02272	0.02463	0.03392	0.03643	0.02888	0.02796
d_p (µm)	60	60	45	45	45	45	45	45
h	4.23	4.58	5.10	5.47	7.54	8.09	6.41	6.21

3.3 Characterisation of CHO supernatant

The protein concentration of the CHO cell culture supernatant was determined by analytical protein A analysis which yielded a mAb concentration of 2.79 mg/mL. This value was verified with another in-house analytical protein A chromatography set-up. However, the value provided by Sartorius was 3.41 mg/mL and was determined with an analytical SEC. In general, it was shown that values obtained with analytical Protein A tended to be about 10% lower than those obtained from spectrophotometric analysis with A 280. Furthermore, the CHO supernatant was analysed for HCP content by an ELISA method and yielded 200 000 ppm. Comparable values have been found by Vikram et al [46]. Analytical SEC showed that the CHO supernatant was already very pure and had a high protein concentration, indicated by the high peak at the mAb retention time. Aggregates and low molecular weight proteins were detected in minor concentration (Figure 12).

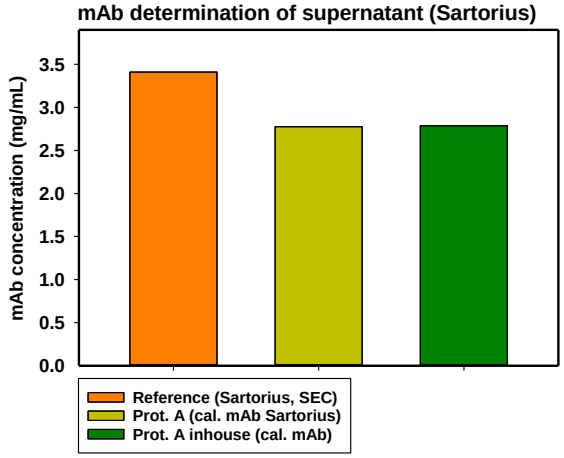

Figure 11: Comparison of methods for determination of mAb concentration in the supernatant

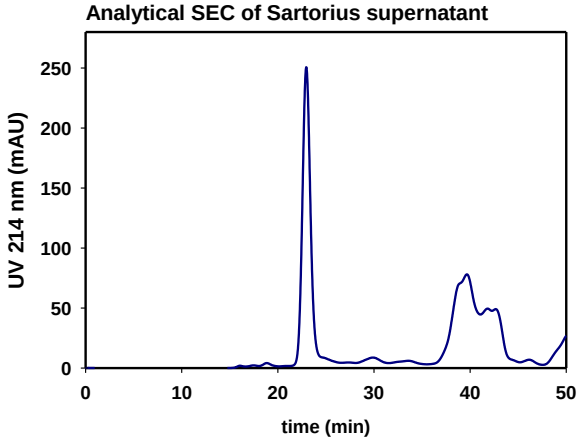

Figure 12: SEC analysis of CHO cell culture supernatant from Sartorius

3.4 Determination of DBC and elution buffer screening

3.4.1 Example of a chromatographic run

In general, every run had a similar sequence of different phases, e.g loading phase, wash out phase, elution phase and regeneration phase. Between the different phases, a wash phase with equilibration buffer was carried out. This was particularly important before the regeneration because of high backpressures when directly switching from acidic to basic pH. In Figure 13 a typical chromatogram comprising the different phases is shown. At the end of the loading step, breakthrough of the mAb can be seen from the shallow increase of the UV 300 nm signal. This breakthrough is dependent on the loading velocity and starts earlier with increasing loading velocity at constant load volume (see section 3.4.3).

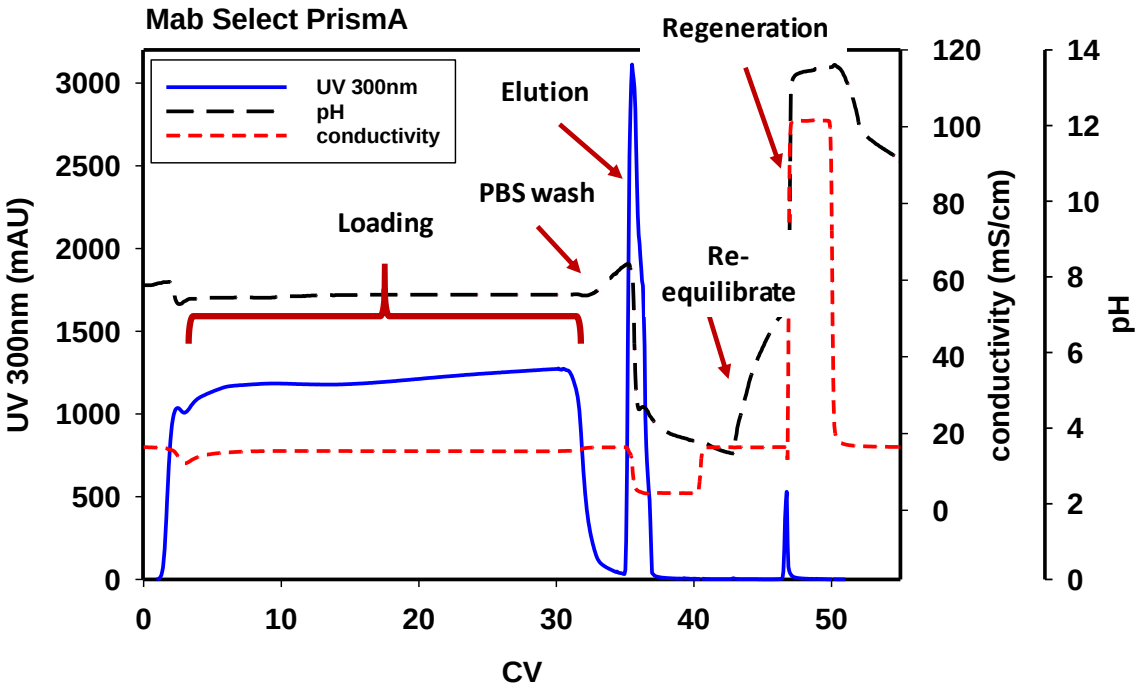

Figure 13: Example of a run of the DBC experiments, carried out with a loading velocity of 300 cm/h and 100 mM citrate at pH 3.2 as elution buffer

3.4.2 Determination of equilibrium bind capacity and recovery

Equilibrium binding capacity and recovery was first estimated by a breakthrough experiment at which the column was completely saturated (Figure 14). 120 mL of CCS were loaded at a velocity of 200 cm/h (residence time ~ 3 minutes), which corresponded to 150 mg mAb loaded per mL resin. After a wash with 5 CV PBS mAb was eluted with pH 3.0 and afterwards the column was stripped with 0.5 M NaOH. The complete BTC as well as the eluate were collected and mAb concentration was determined by analytical Protein A affinity chromatography. For MabSelect PrismA recovery was calculated as:

Equation 27: Calculation of recovery

$$Recovery\ (\%) = \frac{mAb_{FT} - mAb_{El}}{mAb_{load}} = \frac{142.7 + 141.1}{334.8} = 84.7\%$$

If the amount of mAb in the eluate was determined by A280 nm and ε=1.4 a value of 156.5 mg was obtained instead of 141.1 mg and recovery was then 89.3%. For Toyopearl AF-rProtein A HC-650F the corresponding values for the recovery were 80.6 and 88.9 %, respectively. It has to be noted that in these experiments FT collection was terminated at the end of the loading step thus a minor amount of mAb in the wash out was not considered in the mass balance.

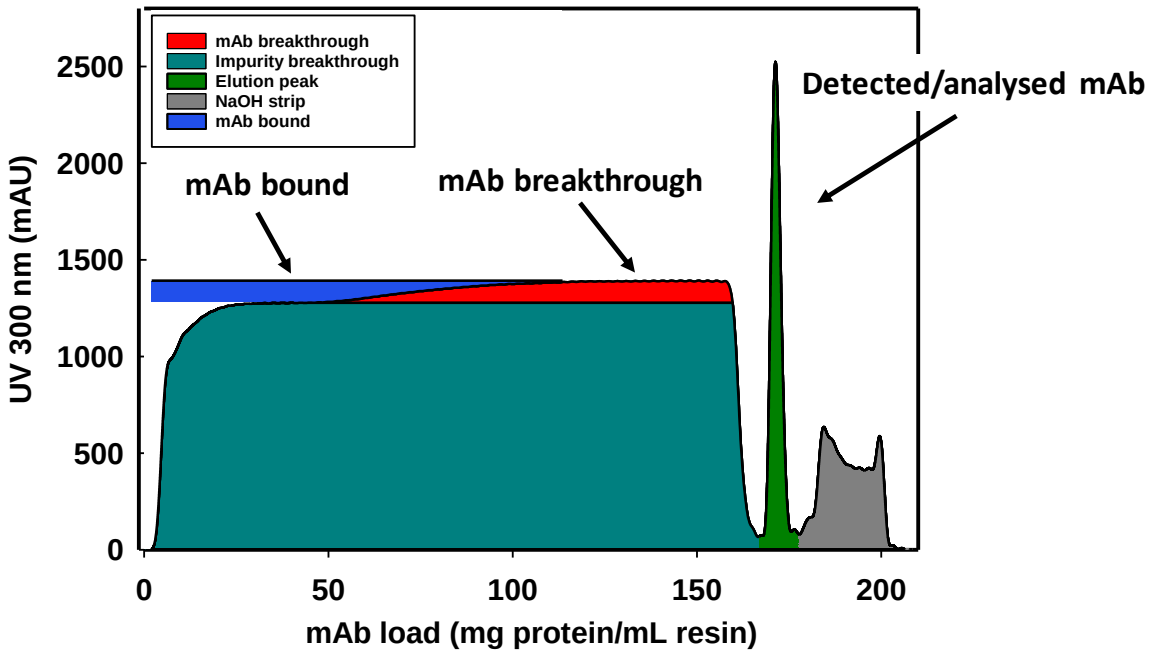

Figure 14: Graphical representation of breakthrough experiment.

Additionally to the determination of mAb concentrations, equilibrium binding capacities were calculated from the break through curves. The absolute absorbance was subtracted by the

contribution of the impurities in the flow through, as indicated in Figure 14. The obtained curve was made dimensionless by normalisation with the absorbance of the pure mAb:

Equation 28: Normalisation with the absorbance of the pure mAb

$$\frac{C}{C_0} = \frac{mAU - mAU_{plateau}}{mAU_{pure\ mAb}}$$

The x–axis was expressed as mg mAb loaded per mL of resin which is obtained by multiplying the volume of loaded supernatant with the mAb concentration and dividing by the resin volume:

Equation 29: Conversion to mg protein per mL resin

$$\frac{\text{mg protein}}{\text{mL gel}} = \frac{V_{CCS} * C_{mAb(\frac{2.79mg}{mL})}}{V_{resin}}$$

Numerical integration of the curve and subtracting the area under the curve from to the total amount of loaded mAb yields the bound mAb per mL of resin corresponding to q_{max}. Using this method a value of 81.4 mg/mL for MabSelect PrismA and 84.0 mg/mL for Toyopearl AF-rProtein A HC-650F was obtained. For comparison of these values with other methods of determination see section 3.5.

3.4.3 Determination of DBC

For the determination of DBC, breakthrough curves with dimensionless concentration (C/C_0) over amount mAb loaded were constructed as outlined in Figure 14 and Equation 28 and Equation 29. 5 different velocities ranging from 75 to 400 cm/h were studied whereat CCS was loaded to reach at least 10% breakthrough (C/C_0=0.1). Overlays of transformed curves are shown in Figure 15. For both resins there was little difference between 75 cm/h and 100 cm/h. DBC dropped more rapidly with increasing velocity for Mab Select PrismA in comparison to

Toyopearl AF-rProtein A HC-650F. This effect can be explained by the smaller particle diameter of the Toyopearl resin.

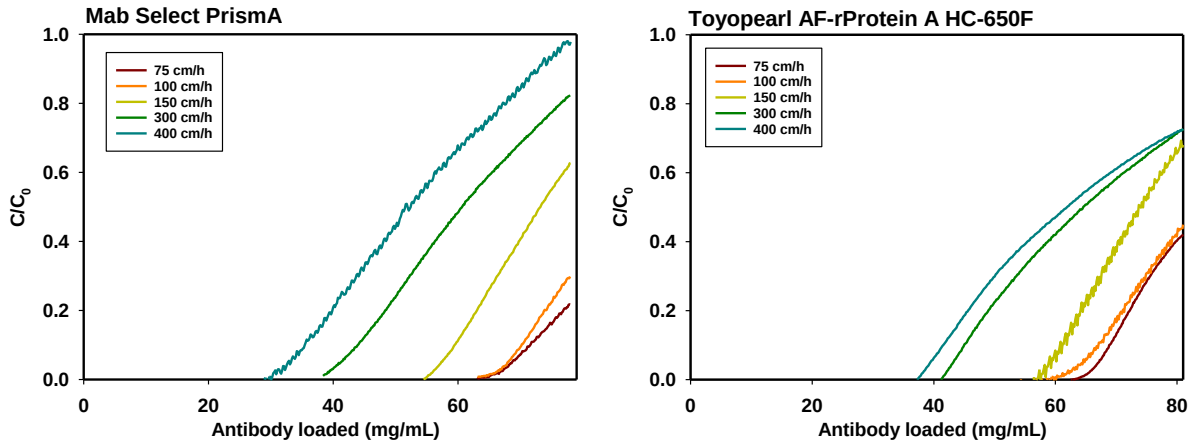

Figure 15: Break through curves with CCS at different velocities

DBC10% values were read at C/C_0=0.1 and plotted against residence time (Figure 16).

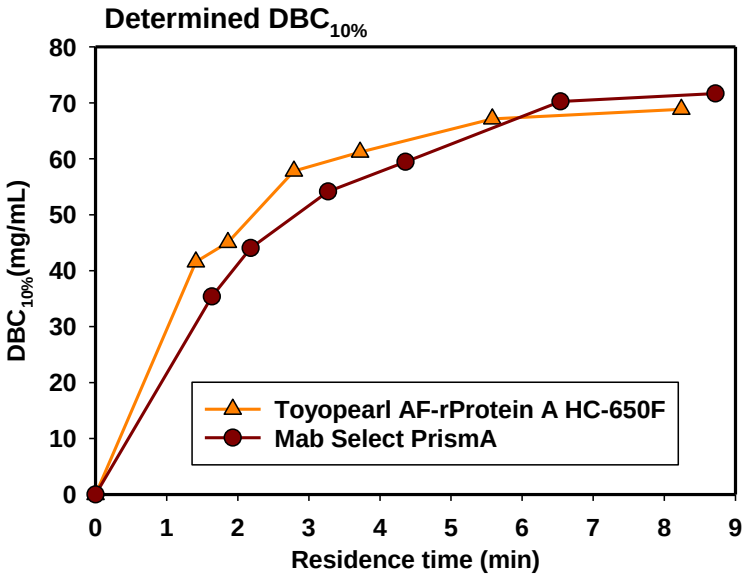

Figure 16: Plot of binding capacities at 10% breakthrough plotted against the residence times

Evidently, the overall faster mass transfer of Toyopearl AF-rProtein A HC-650F is reflected by the slightly faster increase of DBC at higher residence times. Determination of maximal capacities of the reins based on this analysis is shown in Figure 18.

3.5 Determination of pore diffusion coefficient (D_e)

Determination of effective pore diffusion coefficients D_e was based on a pore diffusion model assuming a rectangular adsorption isotherm, which is a reasonable assumption for Protein A affinity chromatography. The model was used in two different ways, first for matching a full breakthrough curve and secondly to determine D_e from $DBC_{10\%}$ data.

3.5.1 Breakthrough curve

The obtained data from the runs which were loaded until fully break through was reached, were converted to C/C_0 and to milligram mAb per millilitre resin. The experimental runs were fitted with a model for column adsorption assuming film and pore diffusion (Figure 17). This model is based on a constant pattern solution and also referred to as the shrinking core model. The model assumes a rectangular adsorption isotherm and is given by Equation 25

$$N_{pore}(1-\tau_1) = +\frac{15}{2} ln\left[1+(1-X)^{\frac{1}{3}}+(1-X)^{\frac{2}{3}}\right] - \frac{15}{\sqrt{3}} tan^{-1}\left[\frac{2}{\sqrt{3}}(1-X)^{\frac{1}{3}}+\frac{1}{\sqrt{3}}\right] - \frac{n_{pore}}{n_{film}}[ln(X)+1] + \frac{5\pi}{2\sqrt{3}} - \frac{5}{2} \quad (25)$$

with

$$\tau_1 = \left(\frac{vt}{L}-1\right)\left(\frac{C_F}{\phi q_F}\right), X = \frac{C}{C_F},\ N_{pore} = \frac{15\phi D_e}{{r_p}^2}\frac{L}{v} \quad (25a)$$

and

$$N_{film} = \frac{3\phi k_f}{r_p}\frac{L}{v}, \phi = \frac{(1-\varepsilon)}{\varepsilon} \quad (25b)$$

In Equation 25 τ_1 is the dimensionless time (-), C the protein concentration (mg/mL), C_F the protein concentration in the feed (mg/mL), q_F the binding capacity at equilibrium with C_F (mg/mL; in case of rectangular isotherm q_F corresponds to q_{max}), v the interstitial velocity (cm/s), t the time (s), L the column length (cm), ε the extraparticle void fraction (-), D_e the effective pore diffusion coefficient (cm^2/s), k_f the film mass transfer coefficient (cm/s), r_p the particle radius (cm) and N the number of transfer units (-).

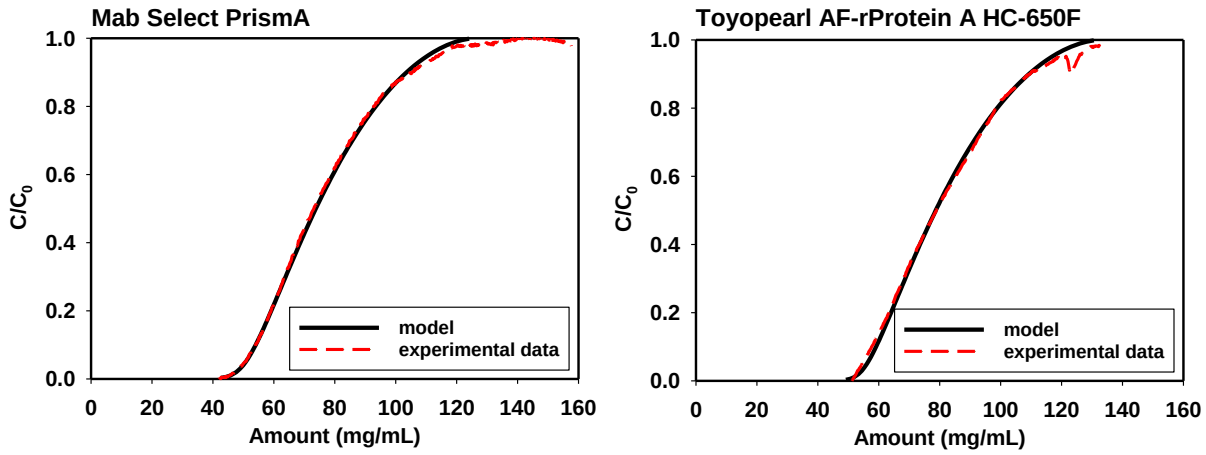

Figure 17: Fit of experimental breakthrough curves with pore diffusion model; running conditions were 200 cm/h

Experimental BTCs performed at 200 cm/h were transformed from time axis into mg mAb loaded per mL resins and fitted with Equation 25. Adjustable parameters were q_m, D_e and k_f. Results are summarized in Table 12.

Table 12: Parameters of fits with pore and film diffusion model

Resin	q_m (mg/mL)	D_e (cm^2/s)	k_f (cm/s)
Mab Select PrismA	75.5	$1.9*10^{-8}$	$2.5*10^{-4}$
Toyopearl AF-rProtein A HC-650F	80.5	$1.1*10^{-8}$	$2.5*10^{-4}$

The capacities obtained are reasonably high. D_e values are relatively small which can be explained by the high density of immobilized Protein A thus leaving little space for fast diffusion in the pores.

3.5.2 Dynamic binding capacity

Another possibility to determine q_m and D_e is evaluate capacity data ($DBC_{10\%}$) with a rearranged form of the pore diffusion model. The feed concentration is small compared to the binding capacity thus Equation (23a) can be expressed as

Equation 30: Simplified expression for the dimensionless time

$$\tau_1 = \left(\frac{vt}{L} - 1\right)\left(\frac{C_F}{\phi q_F}\right) = \frac{DBC}{(1-\varepsilon)q_F} = \frac{DBC}{EBC}$$

where EBC is the equilibrium or static capacity. At $DBC_{10\%}$ C/C_F=0.1 and inserting into Equation 25 and neglecting the last term for film diffusion gives

Equation 20: Constant pattern solution for the dimensionless time at C/C_0=0.1

$$\tau_1 = \frac{DBC}{EBC} = 1 - \frac{1.03}{N}$$

Equation 22 can be used to estimate q_m and D_e from a plot of τ_1 versus N. Since N contains the term L/v it is more convenient to plot τ_1 over residence time.

represents the constant pattern solution which is not valid at very short residence times, but an empirical numerical estimation is available:

Equation 21: General solution for the dimensionless time

$$\tau_1 = 0.364 * N - 0.0612 * N^2 + 0.00423N^3$$

DBC data shown from Figure 16 were plotted and fitted with Equation 22 and Equation 23. The plots are shown in Figure 18 and fitted parameters are listed in Table 13.

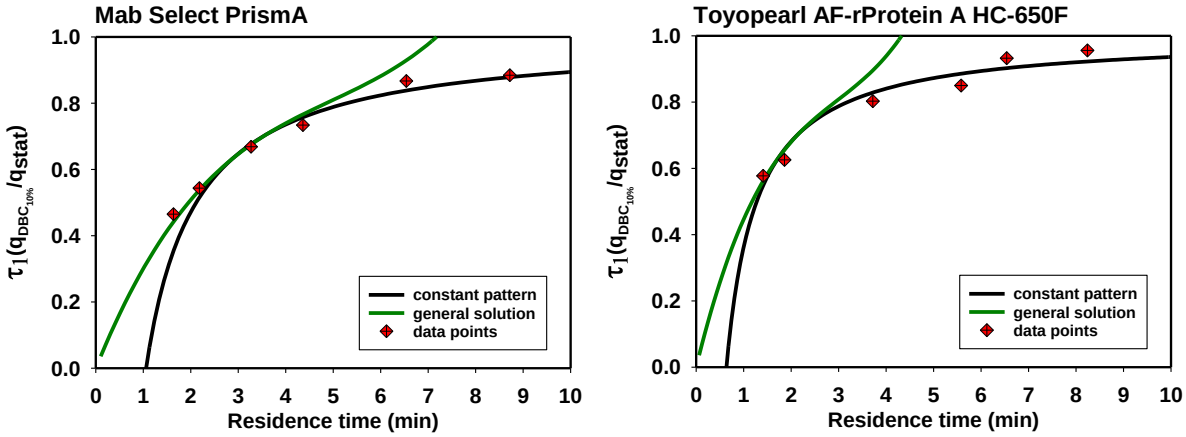

Figure 18: Fit of DBC vs. residence time data with rearranged pore diffusion model.

Table 13: Parameters of fits with pore diffusion model

Resin	q_m (mg/mL)	D_e (cm^2/s)
Mab Select PrismA	81.0	$1.5*10^{-8}$
Toyopearl AF-rProtein A HC-650F	72.0	$1.4*10^{-8}$

The values for D_e only differ slightly from those obtained from fitting the whole breakthrough curve. The values are in reasonably good agreement with those obtained by Papst et al [34]. Comparing the two types of analysis regarding q_m, the value for MabSelect PrismA is higher for the $DBC_{10\%}$ analysis while for Toyopearl AF-rProtein A HC-650F it is reverse. The reason for this discrepancy lays in the fact that it is difficult to reach full breakthrough and secondly that there are always slight drifts in UV absorbance over the time course of the experiments. Thus the normalisation in terms of C/C_F is affected with some error that can be leading to different results. It is fair to take any average value of both determinations and state that q_m is equally high at ~76-79 mg/mL for both resins. However, regarding DBC, Toyopearl AF-rProtein A HC-

650F performed slightly better due to the smaller particle diameter as shown in Figure 15-Figure 17.

3.5.3 Prediction of breakthrough curves

Theoretical break through curves, based on averaged values for D_e were constructed and are shown in Figure 19. These curves were used to predict the breakthrough profiles for prospective experiments and experiments, e.g. the amount of loaded mAb were planed based on this model graphs. The loading for the experiments were designed to reach approximately 90% of the maximum load at given velocity without any breakthrough. Furthermore, it can be observed that both resins have a similar behaviour concerning their effective diffusion coefficient and their dynamic binding capacity. Comparing the obtained results with those obtained for previous stationary phases it is obvious that resins like Mab Select SuRe or ProSep-vA Ultra show around 4 times higher D_e than the resins investigated in this study. On the other hand, their static binding capacity is about 40% lower. Particles radii of the older generation was around d_p=~75-100 µm [39]. In contrast, the MabSelect PrismA and Toyopearl AF-rProtein A HC-650F have a d_p of 60 and 45µm, respectively. It can be concluded that these resins compensate their low diffusion coefficient by a high binding capacity due to high ligand density and the use of smaller particles to enable efficient mass transfer.

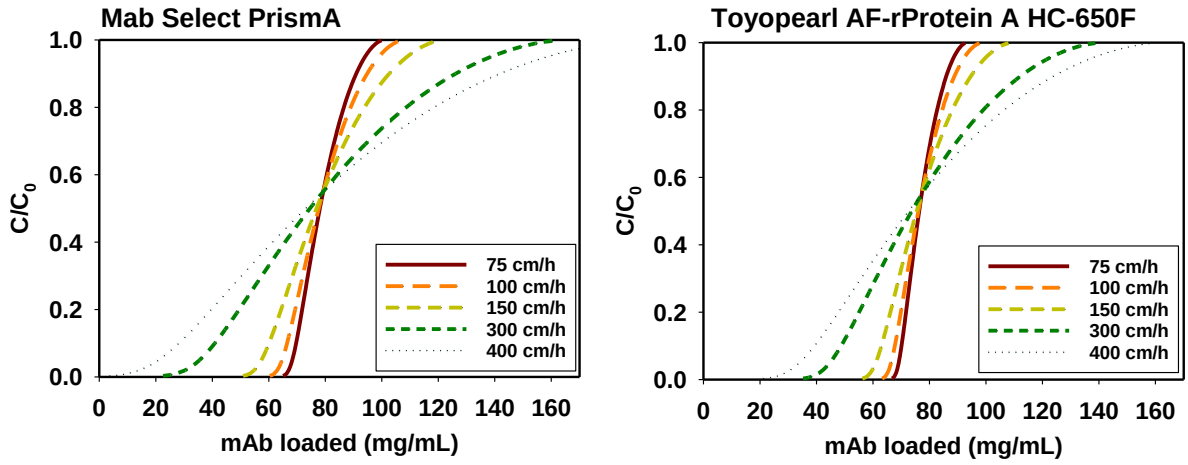

Figure 19: Predicted breakthrough curves generated from the fit of the constant pattern solution. Assumed average values were q_m = 78.3 mg/mL, D_e=1.7*10^{-8} cm^2/s for MabSelect PrismA and q_m = 76.3 mg/mL, D_e=1.25*10^{-8} cm^2/s for Toyopearl AF rProtein A HC-650F.

3.5.4 Elution profiles of tested buffers

In the course of the experiments for determination of DBC, a preliminary testing of elution buffers was carried out. Elution pH was varied between pH 2.9 and 3.2; furthermore, different buffer species and concentrations were tested. Tested elution buffers were 25 mM HAc pH 3.2 and 100 mM HAc pH 2.9; 100 mM sodium citrate at pH 3.0 and 3.2 respectively, and 100 mM glycine/HCl at pH 3.0. An overlay of the elution profiles is shown in Figure 20. In general, both resins exhibited similar profiles for the respective buffers. A slight trend towards smaller elution volumes for Toyopearl AF-rProtein HC-650F can be observed. 100 mM HAc pH 2.9 showed the narrowest and 100 mM glycine/HCl at pH 3.0 the broadest peaks. For Toyopearl AF-rProtein HC-650F the profile with HAc is pH 3.2 significantly broader than the corresponding one on MabSelect PrismA. Probably, the low molarity of this buffer (25 mM) is the reason for this behaviour. Citric acid absorbs at a wavelength of 340 nm, which can disturb protein determination at 280 nm and can be regarded as a certain drawback for using this buffer.

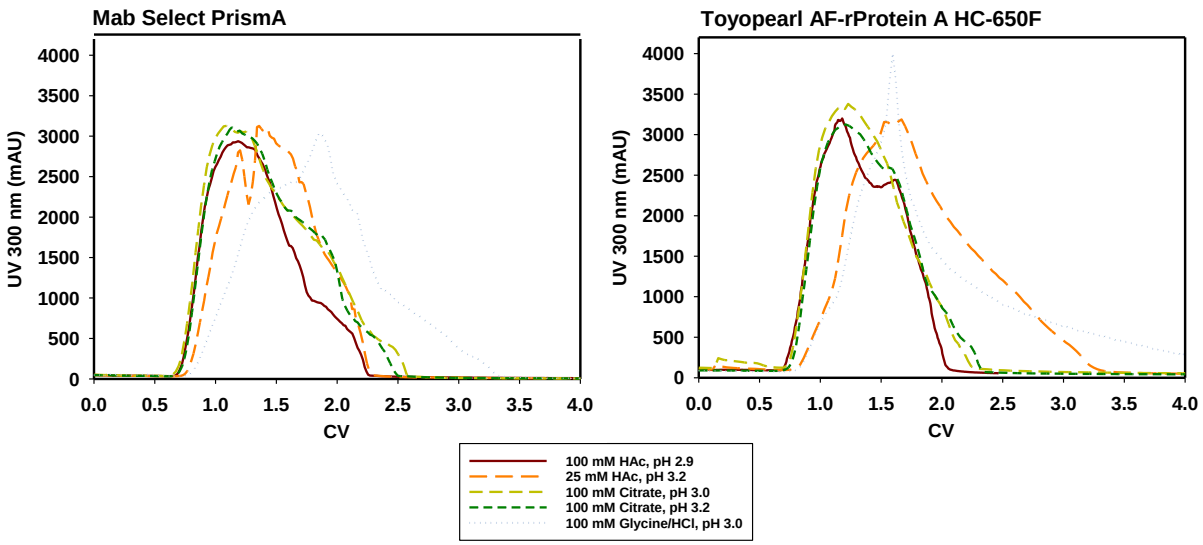

Figure 20: Elution profiles obtained with different elution buffers

In summary, the mAb eluted between 1-2 CV for all the tested buffers, which is an acceptable range. Only the glycine buffer at pH 3.0 did not show sufficient elution power.
As a compromise, a buffer consisting of 56 mM HAc pH 3.0 was chosen as the standard elution buffer for all upcoming experiments.
In Figure 21 the mAb concentrations in the eluates are shown. In principal, these values reflect the width of the elution peak in a reverse manner.

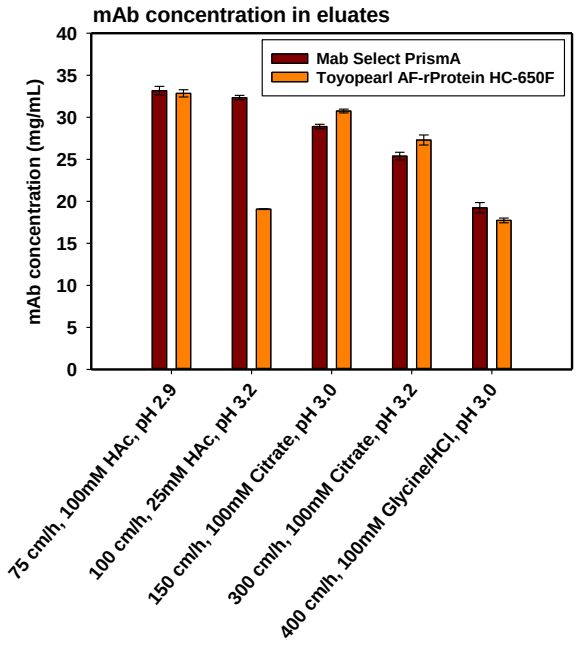

Figure 21: mAb concentrations of eluates generated within the buffer screening experiments

3.5.5 CHO-HCP ELISA of DBC Experiments

Samples from the elution buffer screening were analysed for HCP content. The ELISA results show that the HCP content could be reduced by a factor of 50-100 compared to the input concentration of the cell culture supernatant. In general, fractions purified with Mab Select PrismA showed two-fold lower HCP content than those purified with Toyopearl AF-rProtein A HC-650F. The loading velocity and the elution buffer did not show a significant impact for Mab Select PrismA. In contrast, a trend of reduced HCP content with increasing loading velocity could be observed for the Toyopearl AF-rProtein A HC-650F resin. Previously, it was shown that there is interaction of HCP directly with the mAb, which is probably also the case in these experiments [27]. Therefore, it is possible that the HCP-mAb interaction is favoured at low loading velocity because there is a higher residence time on the column and consequently more time for the interaction. On the other hand, Mab Select PrismA did not show this effect which could also indicate that the resin material holds an important role. Other studies indicate that there can be binding interactions between the chromatographic resin and various HCPs [31, 32]. However, in the experiments for DBC determination and initial elution buffer screening, resins were significantly overloaded to obtain a breakthrough. This fact makes the interpretation of the results difficult because HCP content is dependent on two factors, the mAb concentration and the HCP concentration. Further experiments at realistic loading conditions that are without mAb breakthrough, are probably more significant and are described in the following sections.

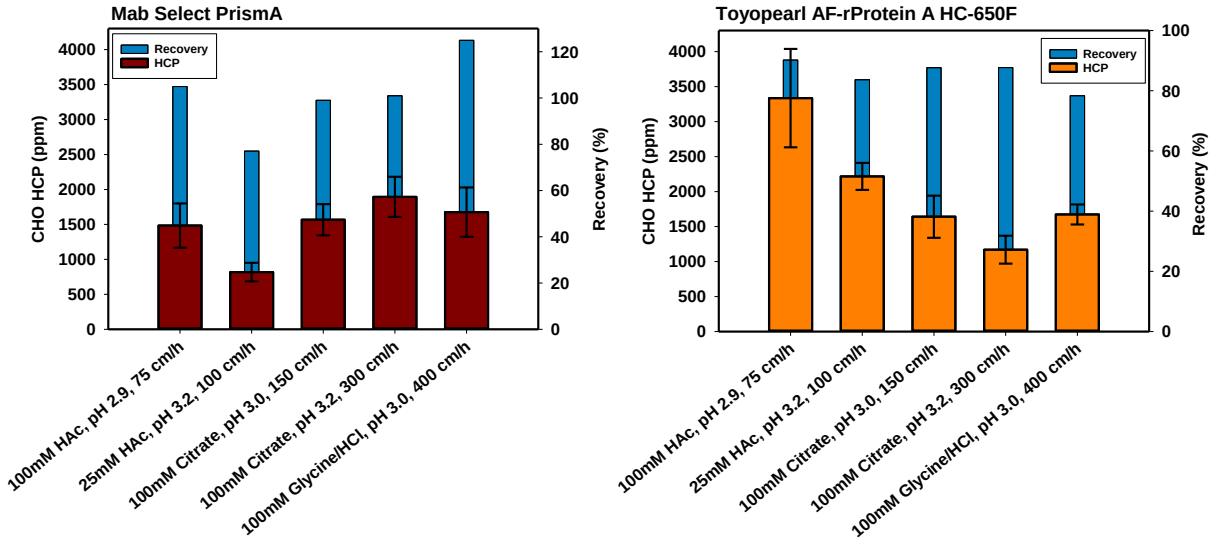

Figure 22: HCP content and recovery generated in the buffer screen experiments

3.5.6 SEC results of various buffers

Eluates were analysed by analytical SEC using a Superdex 200 increase column. As shown in Figure 23, aggregate formation did only occur to a very limited extent, regardless of the used elution buffer. This behaviour was common to both Protein A resins. It is supposed that aggregate formation occurs predominantly when eluting at low pHs or storing the mAb at low or high pH. Furthermore, repeated temperature change can also support aggregation [47-49]. Other studies have also shown that the velocity of elution does not play a big role in aggregate formation but that the elution pH contributes to an high extent to the formation of aggregates [50]. However, none of the above-mentioned mechanisms applied to the mAb used in this study. Monomer content was constantly > 98%, even for repeated freeze and thaw cycles (data not shown).

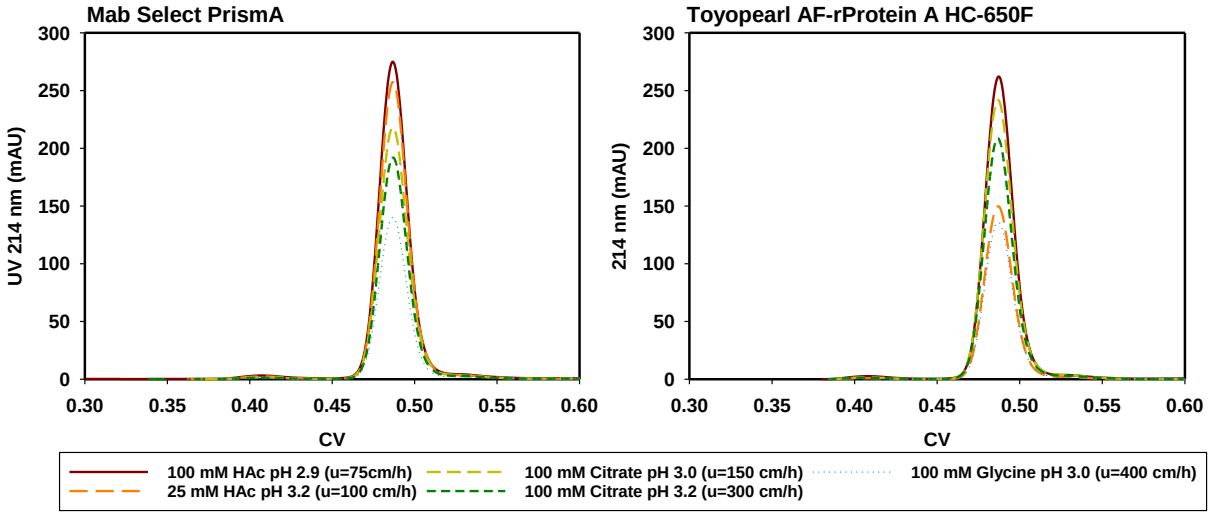

Figure 23: Comparison of SEC runs of eluates generated in the buffer screen experiments

3.6 Variation of mAb loading and loading velocity

The initial idea behind this set of experiments was to test whether i) the total amount of mAb and ii) the distribution of the mAb along the column has an influence on aggregation during elution and also on HCP removal. Therefore, the experiments were designed in a way to achieve three levels of resin saturation, at which both resins were loaded to approximately 90% of possible saturation without breakthrough. This was achieved by loading at three different loading velocities, 100, 200 and 400 cm/h, respectively. Variation of the saturation was achieved by keeping the loading velocity constant at 100 cm/h and applying three different amounts of mAb, which were based on the amounts loaded in previous experiments. All other parameters were kept constant to achieve comparability. The elution buffer was selected to be acetic acid with a pH of 3.0, which corresponds to a concentration of 56 mM.

3.6.1 Example run for this series of experiments

In Figure 24 a representative chromatographic run is shown. At the beginning of elution pH (black curve) goes down steeply and later levels out at a pH of approximately 4. This can be explained that by the fact that acetic acid has a pka value of 4.76 and therefore holds the biggest capacity at this pH range. The low conductivity during the elution indicates the low salt content of the elution buffer, as it was only acetic acid and not acetate buffer. The elution sequence is completed by a wash with equilibration buffer and regeneration with NaOH. After that a re-equilibration step is carried out

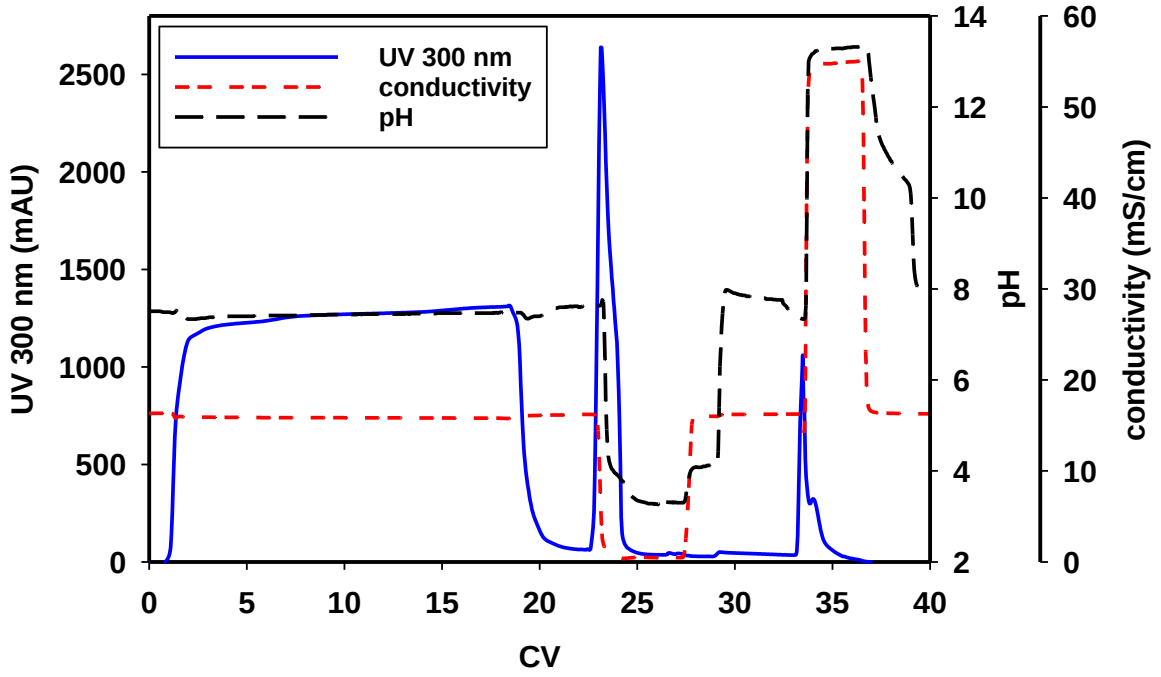

Figure 24: Typical chromatogram without breakthrough for Toyopearl AF-rProtein A HC-650F, u=100cm/h and saturation= 65mg/mL

3.6.2 Elution profile and recovery of variation of loading and loading velocity

Elution profile overlays were arranged to represent different loading velocities (Figure 25) and different saturation at constant velocity of 100 cm/h (Figure 26). The obtained recoveries ranged from 70 to 100%, at which the runs with low saturation had the lowest recovery. This was especially evident for the Toyopearl resin. Concerning the elution peaks, the same trend could be observed for both resins. Clearly, the amount of loading had a significant effect on the retention time. High loadings reduced the start of the elution peak at about 0.75 CV compared to 1.2 CV at low saturation. This phenomenon is in line with common theory of chromatography.

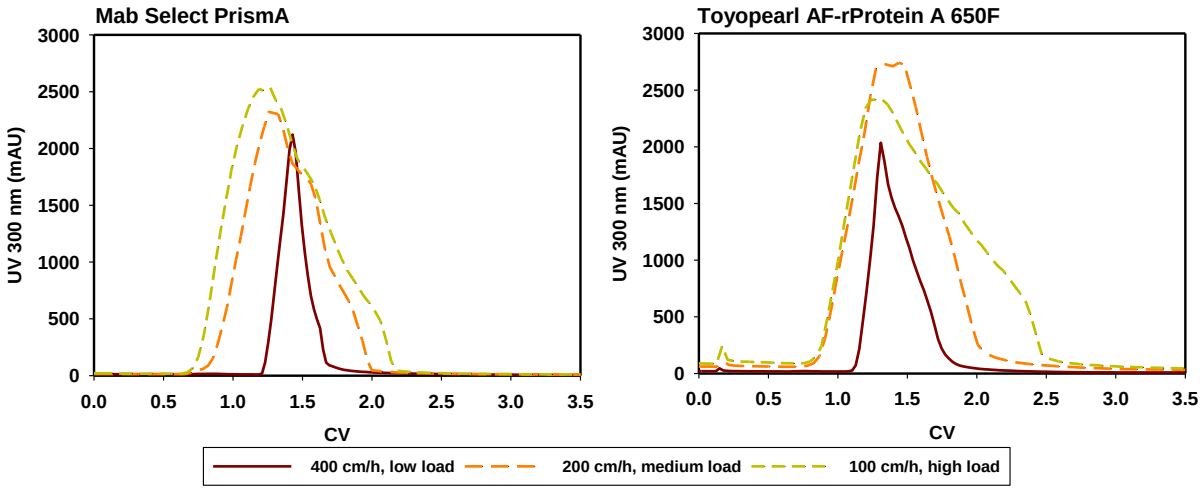

Figure 25: Elution profiles obtained with different loading velocities

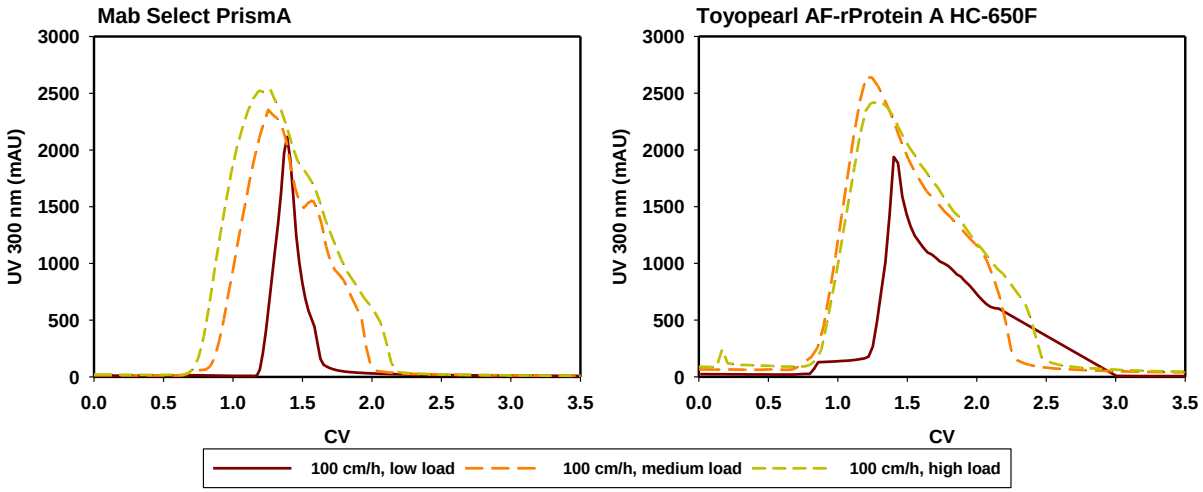

Figure 26: Elution profiles obtained with different amounts of mAb loaded

3.6.3 SEC of fractions from variation of loading and loading velocity

In Figure 27 analytical SEC results are shown. Similar to previous results, no aggregation could be detected at any conditions. This result is in contrast to published results showing that higher loadings might induce aggregate formation due to denser contact of neighbouring proteins or amino acids [50]. However, the mAb used in this study seems to be characterized by an exceptionally high stability.

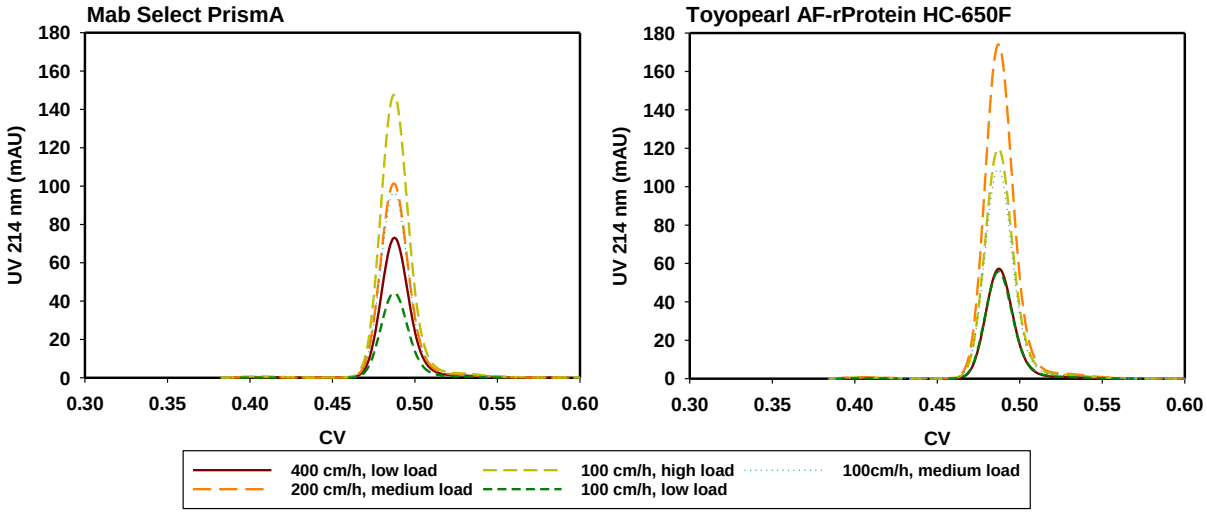

Figure 27: Comparison of SEC results of variation of loading and loading velocity

3.6.4 CHO-HCP ELISA of variation of loading and loading velocity

In Figure 28 HCP results are shown for variation of velocity. A clear trend to higher HCP levels at higher velocities, which in turn leads to lower saturation, can be observed. This trend is more pronounced for Toyopearl AF-rProtein A HC-650F. In general, the lowest HCP content was detected at high load and low loading velocity for both resins. When comparing these results to those from the DBC experiments the opposite trend was found (in DBC experiments the HCP content was lower at higher velocities). A possible explanation is that in the DBC experiments the resins were overloaded with the same amount of protein. Hence, protein saturation was highest at 75 cm/h and lowest at 400 cm/h, but still higher for 400 cm/h compared to this set of experiment. Possibly, the ratio of mAb to HCP is the most important factor. In the DBC experiments the resins were overloaded, therefore mAb that could not bind anymore ran through but this does not apply necessarily for HCPs. Low flow velocities could promote this additional loading of HCP because the HCP interactions may decrease with velocity. The value obtained in the loading experiments at 400 cm/h might be higher because at this velocity there is few mAb bound on the column which could generate extra space for mAb-HCP interaction or HCP-resin interaction. This could explain why the lowest value for both columns was obtained at 100 cm/h and high saturation.

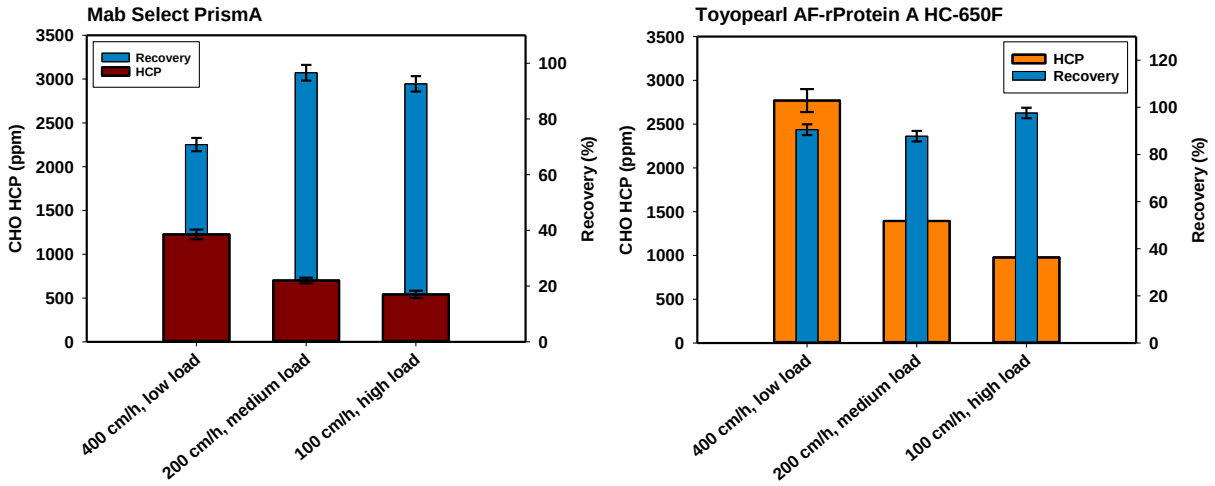

Figure 28: HCP content and obtained recovery of variation of loading velocity experiments

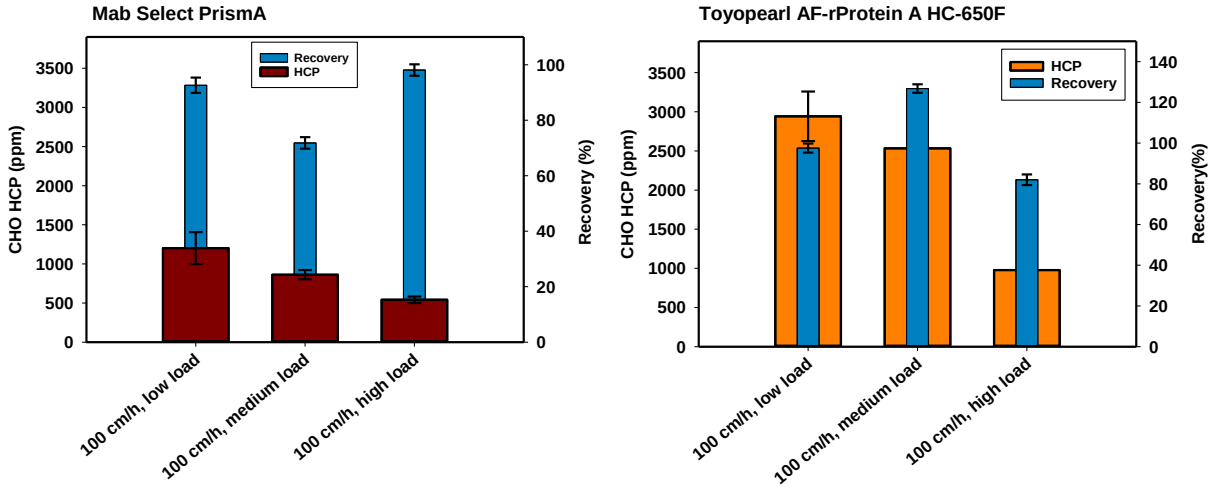

Figure 29: HCP content and obtained recovery of variation of load experiments

When only the amount of mAb loaded was considered the same correlation of high HCP at lower saturation could be observed (Figure 29). Other studies have shown that the load of mAb does not have an effect on the HCP content but that the ratio of mAb and HCP in the supernatant has a high effect [46]. Evaluating this factor for this study was not possible as there was no null supernatant (without mAb) available for spiking experiments. Therefore, further research would be needed to study this influence. Summarising, it can be concluded that the loading velocity was a more significant factor for Toyopearl AF-rProtein A HC-650F resin than for Mab Select PrismA.

3.7 Variation of elution velocity

In this set of experiments the elution velocity was varied, other parameters were kept constant.

3.7.1 Example run for the variation of elution velocity

In Figure 30 a representative run at an elution velocity of 200 cm/h is shown. Like in previous runs, after elution a wash with PBS and alkaline regeneration was carried out.

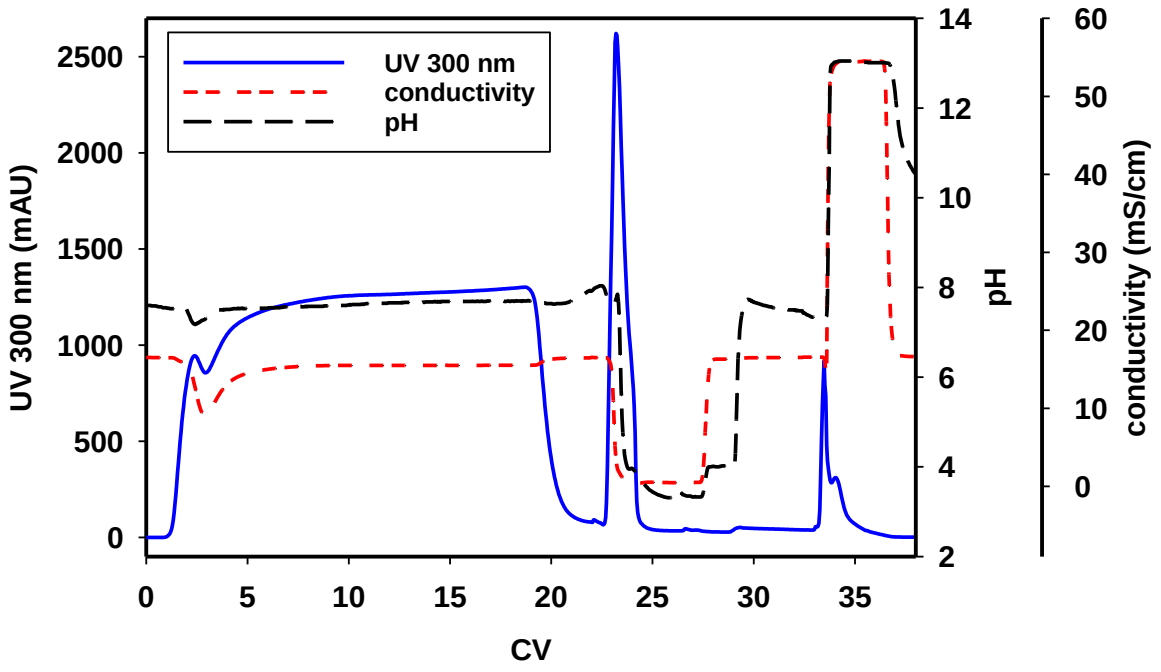

Figure 30: Example of variation of elution velocity of Toyopearl AF-rProtein A HC-650F, $u_{elution}$=200 cm/h

3.7.2 Elution profile at different elution velocities

Overlays of elution profiles are shown in Figure 31. In general, higher velocity leads to broader peaks. However, for Toyopearl AF-rProtein A HC-650F this trend was much more pronounced despite the fact that it has a smaller particle size compared to MabSelect PrismA.

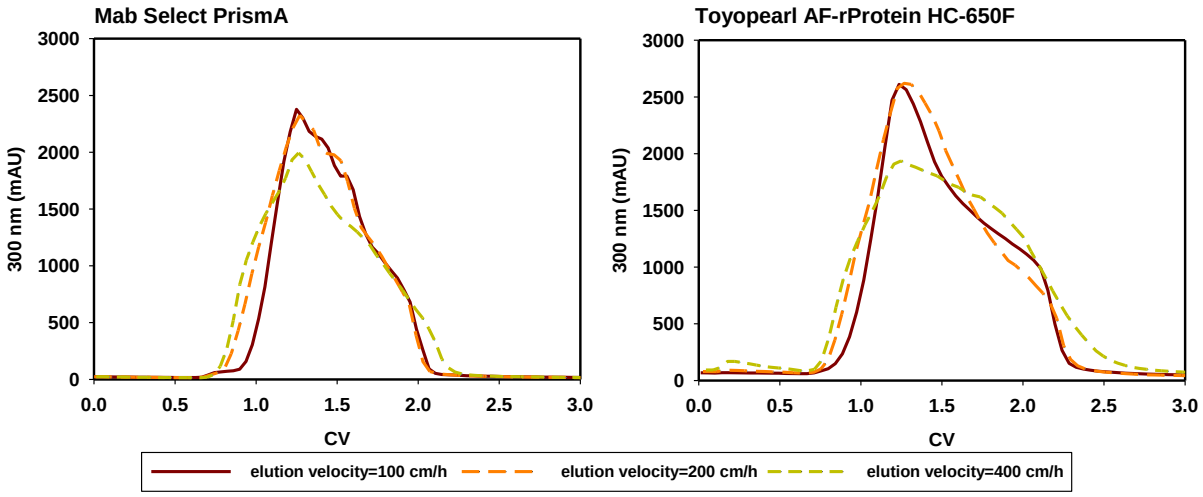

Figure 31: Elution profiles obtained in the variation of elution experiments

3.7.3 SEC results of the experiments of the variation of elution velocity

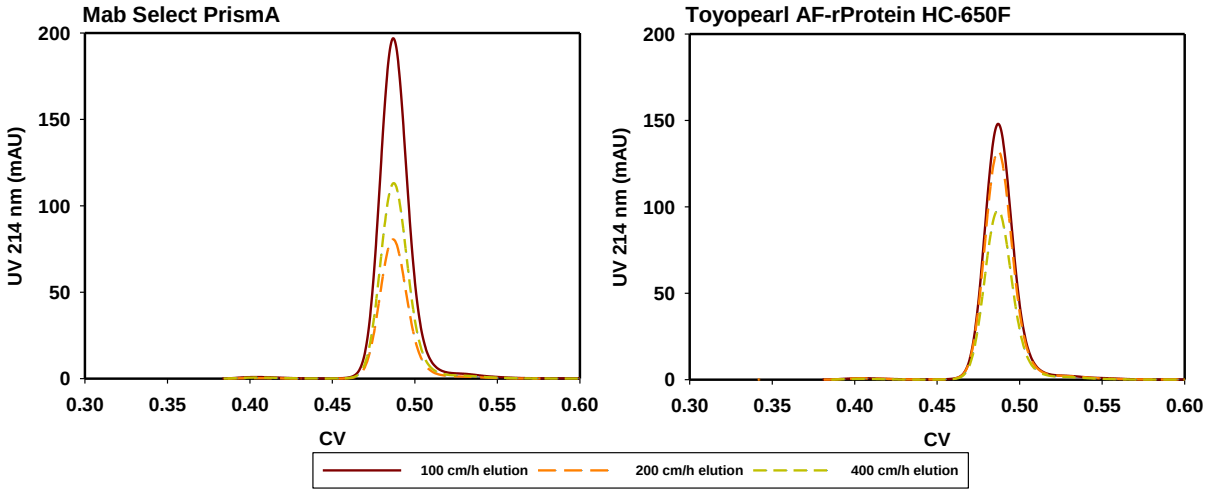

Figure 32: SEC results of eluates obtained in the variation of elution velocity experiments

As shown in Figure 32, aggregate formation due to variation of the elution velocity did not occur. Clearly, the mAb concentration in the Toyopearl AF-rProtein A HC-650F eluates was much smaller due to the substantially broader peaks.

3.7.4 HCP content for the variation of the elution velocity

Although the protein concentration of the eluted fractions showed an influence due to peak broadening, this did not affect the HCP content as it is shown Figure 33. In this set of experiments, the load was kept constant at 90% of possible load without break through. Comparing the values from this experiment to the ones of the variation of loading, similar HCP values were obtained for both columns (see section 3.6). Recovery was constantly high throughout all tested velocities.

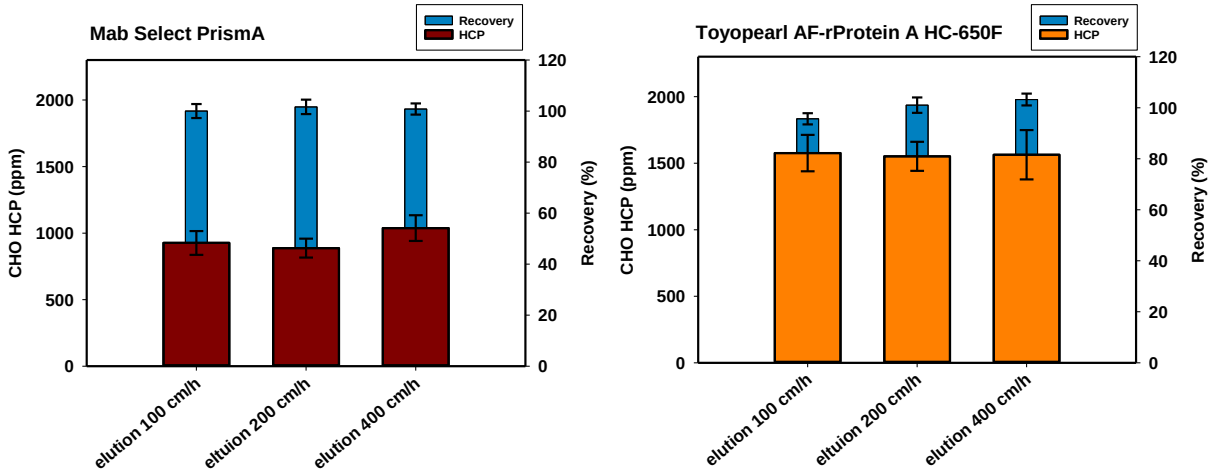

Figure 33: HCP content and recovery of obtained eluates generated in the experiments of variation of elution velocity

3.8 Introduction of a pre-elution step and variation of velocity

In this set-up of experiments, a pre-elution step at slightly acidic pH was introduced to remove HCP content in the actual elution step. Preliminary experiments were conducted to specify the pH of the buffer. For both resins, a 3 CV wash with a 50 mM citrate buffer was applied, the pH was 5.0 for MabSelect PrismA and 4.8 for Toyopearl AF-rProtein A HC-650F, respectively. Velocities for the pre-elution steps were 100, 200 and 400 cm/h.

3.8.1 Example runs including a pre-elution step

In Figure 34 a representative run including pre-elution step is shown. This step was introduced after washing out of unbound sample with 1xPBS and elution was carried out directly after the pre-elution. In some chromatograms small peaks at the pre-elution steps were observed. SEC results showed that this peaks mainly contained mAb but overall the amount was negligible. The effect of the pre-elution is visible in the chromatogram by the drop of pH and conductivity. Furthermore, a slight pH overshoot within the start of the pre-elution can be observed which was less pronounced compared to elution with acetic acid at pH 3.0 without pre-elution at pH 5.0.

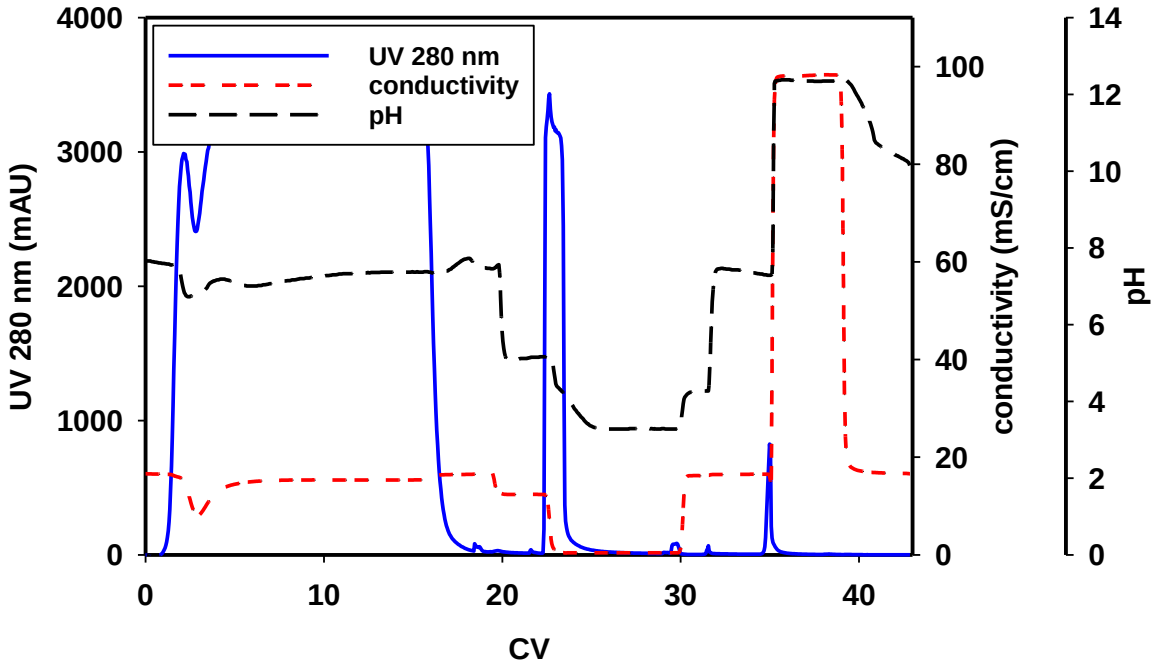

Figure 34: Example of a run including a pre-elution step for Mab Select PrismA with 50 mM citrate buffer pH 5.0 and an elution velocity of 200 cm/h

3.8.2 Elution profiles of pre-elution steps

Additional monitoring at UV 280 was included to be able to detect also weak signals of proteins in the pre-elution step. Overlays of elution peaks are shown in Figure 35. Surprisingly, notable signals could only be observed at the highest velocity of 400 cm/h. However, in terms of recovery the amounts of eluted protein were negligible and did not influence the overall recovery.

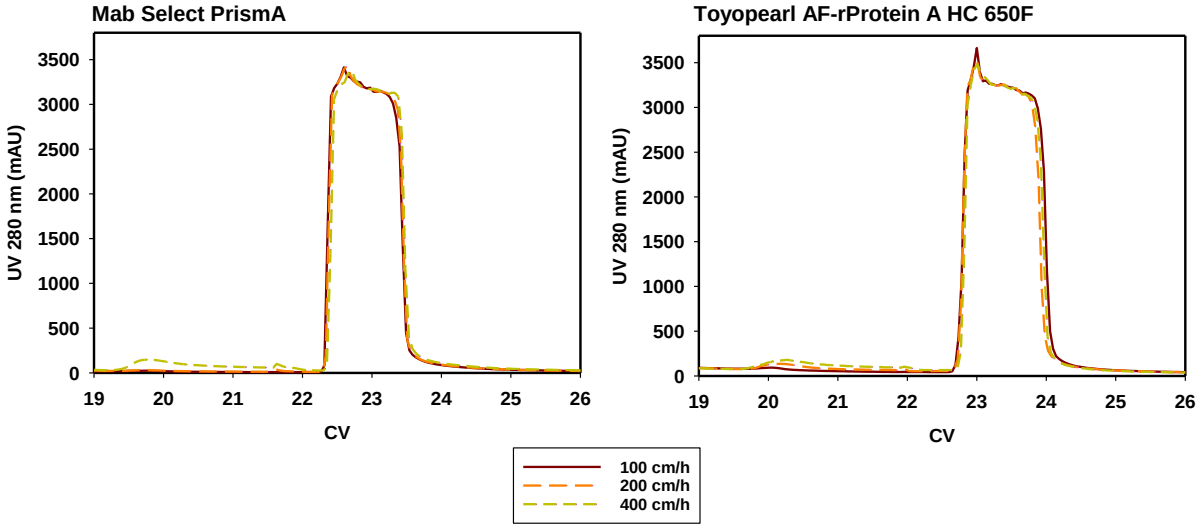

Figure 35: Elution profiles of experiments from variation of pre-elution velocity

3.8.3 SEC results of pre-elution experiments

Like in the previous experiments, aggregation could not be detected as shown in Figure 36. However, other studies have shown that such a pre-elution could reduce aggregation due to a stepwise pH reduction instead of a direct elution with low pH [50].

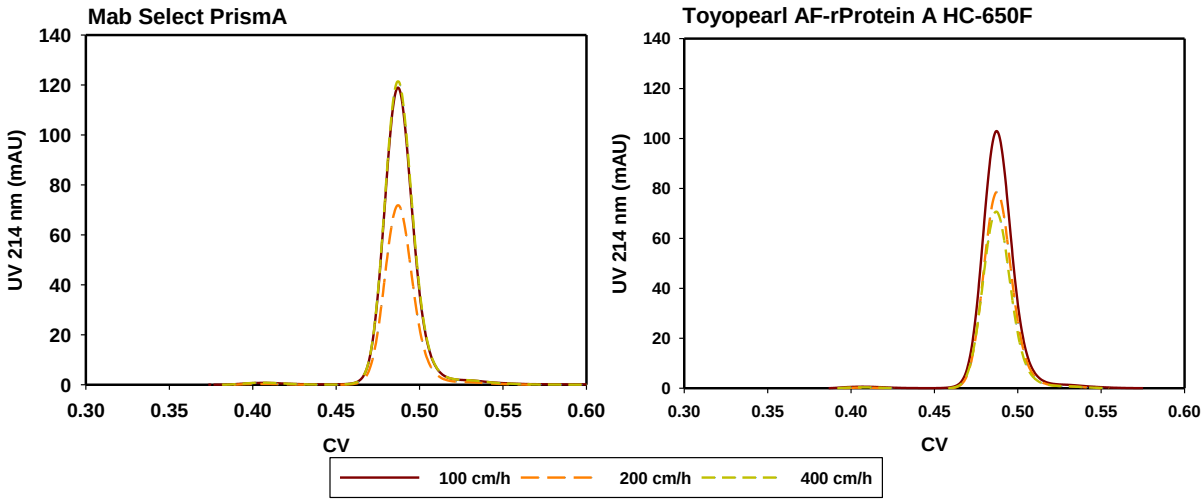

Figure 36: Comparison of SEC results from variation of pre-elution velocity always 3 CV

3.8.4 HCP content for pre-elution experiments

The introduction of a pre-elution step did not reduce the HCP content of the eluted fraction, as can be seen in Figure 37. One run with same amount of mAb loaded and without pre-elution step was used as reference value. Also, velocity of this step did not have any impact. This result is very surprising because Shukla et al have shown in their work that a pre-elution step can significantly reduce the HCP content [32]. However, different studies show that there is high variability of HCP levels at different elution buffers, resins and different supernatants. Furthermore, in comparison to the other studies, values of HCP contents obtained in the current experiments are already in a relatively low range [46].

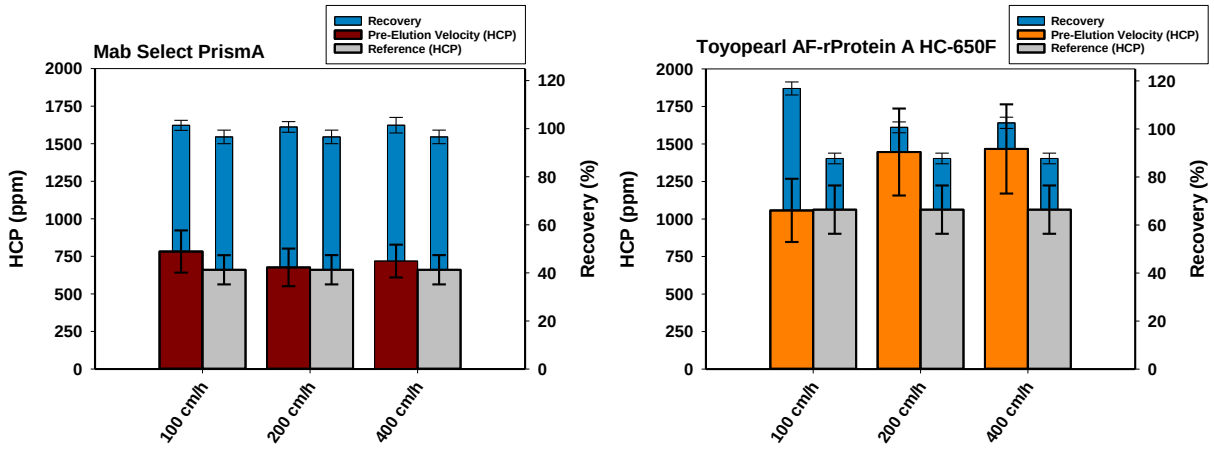

Figure 37: HCP content and recovery of eluates generated in the pre-elution experiments which are compared to a reference value which was generated with the same conditions without pre-elution.

3.9 Implementation of an intermediate wash for the reduction of HCP

In the final, most advanced test series, an intermediate wash step was introduced in addition to the pre-elution step. Buffer conditions were 20 mM TRIS/HCl at pH 9 with 10% isopropanol and 1 M urea. This buffer had previously been shown to be very effective by Shukla et al[32]. This step was incorporated between the PBS wash after sample load and before the start of the pre-elution. This strategy reduces the chance of precipitating salts or proteins due to very high pH differences. The influence of the intermediate wash on the HCP content was investigated by varying the washing velocity and the wash intensity, or time of contact respectively. Velocities were 100 and 400 cm/h using 4 and 8 column volume washes, respectively.

3.9.1 Example run including an intermediate wash

A typical chromatography run comprising of an intermediate wash step, a pre-elution step and an elution step at pH 3.0 is shown in Figure 38. These steps are represented by three peaks which appeared in every run. The intermediate wash step is characterized by a rise of pH and drop of the conductivity and also higher backpressures due to the inclusion of 10% Isopropanol.

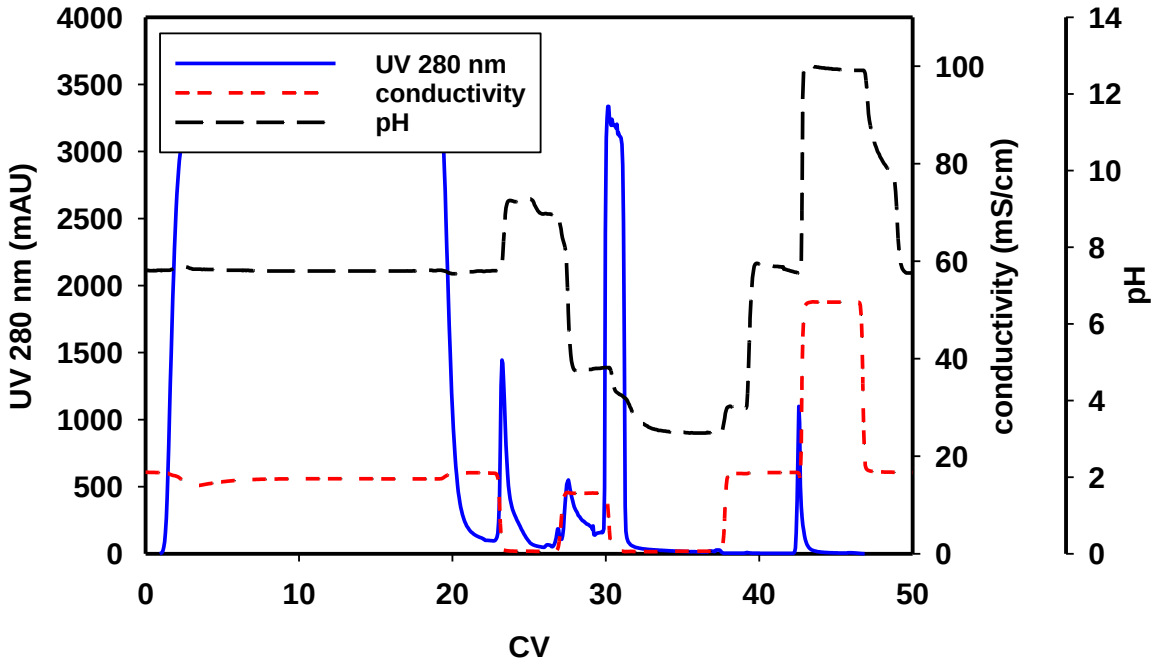

Figure 38: Example of a run including an intermediate wash for Toyopearl AF-rProtein A HC-650F with 400 cm/h and 4 CV

3.9.2 Elution profile within the intermediate wash

In Figure 39 profiles of the intermediate wash step and the pre-elution step are shown. The profiles are characterized by three distinct peaks. The large one stems from the intermediate wash step and the two smaller ones from the pre-elution step. The obtained peaks indicate that some proteins are washed out of the column, but the recovery was not influenced markedly through this wash. Furthermore, the effect of the velocity is visible due to peak broadening of the intermediate peak. The amount of wash buffer and the number of CV had no influence on this washing peak which is visible in the chromatogram because this impurity peak always elutes approximately within three CV for both columns, independent of velocity and amount of washing agent. In all chromatograms, there are also peaks within the pre-elution visible that are probably mAb signals and interferences of the 10% isopropanol in the buffer change.

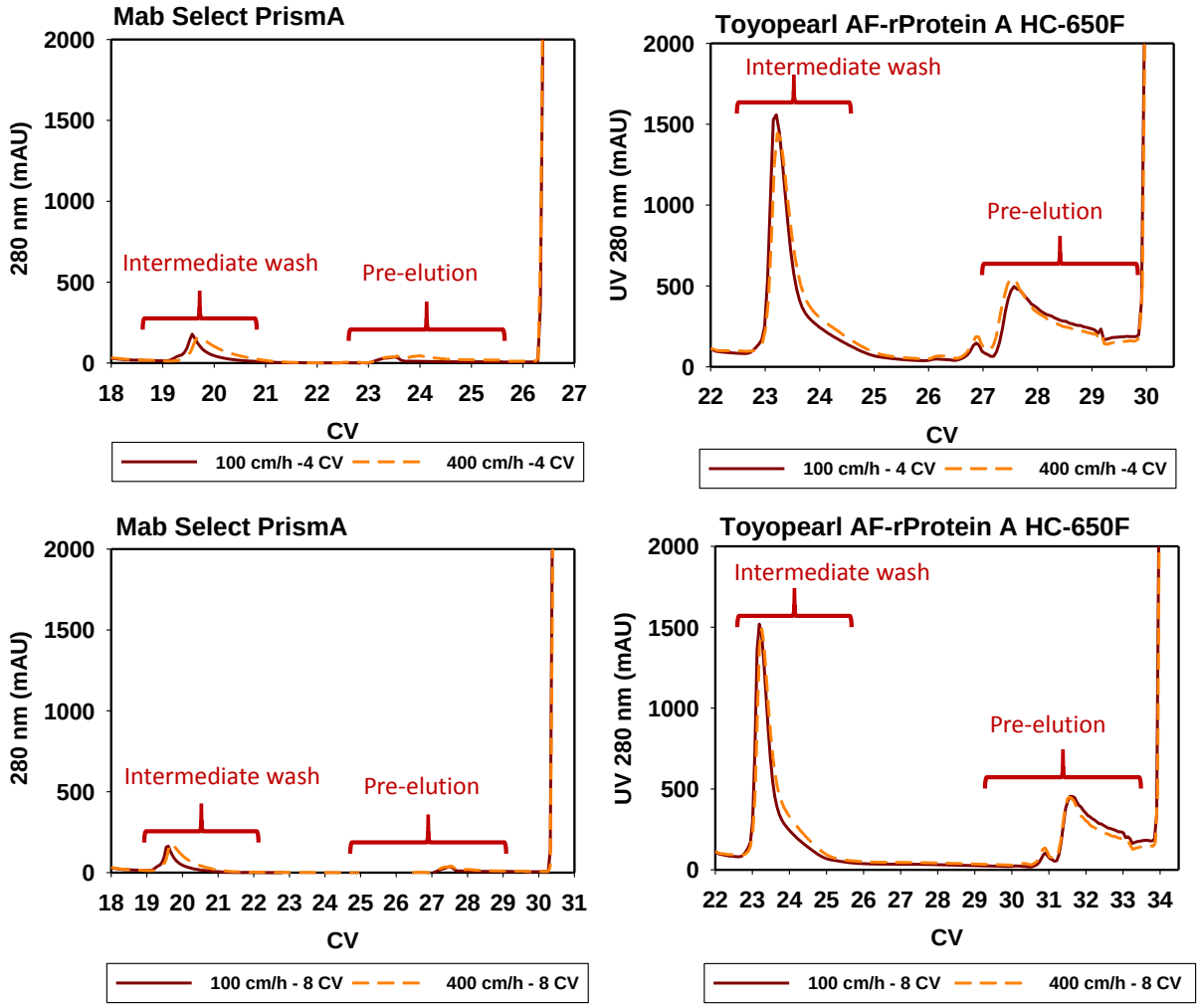

Figure 39: UV profiles of intermediate wash step and pre-elution.

3.9.3 SEC results for the experiments of the intermediate wash

Just as in the experimental set-ups described before, no aggregation could be detected by analytical SEC (Figure 40).

3.9.4 CHO-HCP ELISA after implementation of a intermediate wash

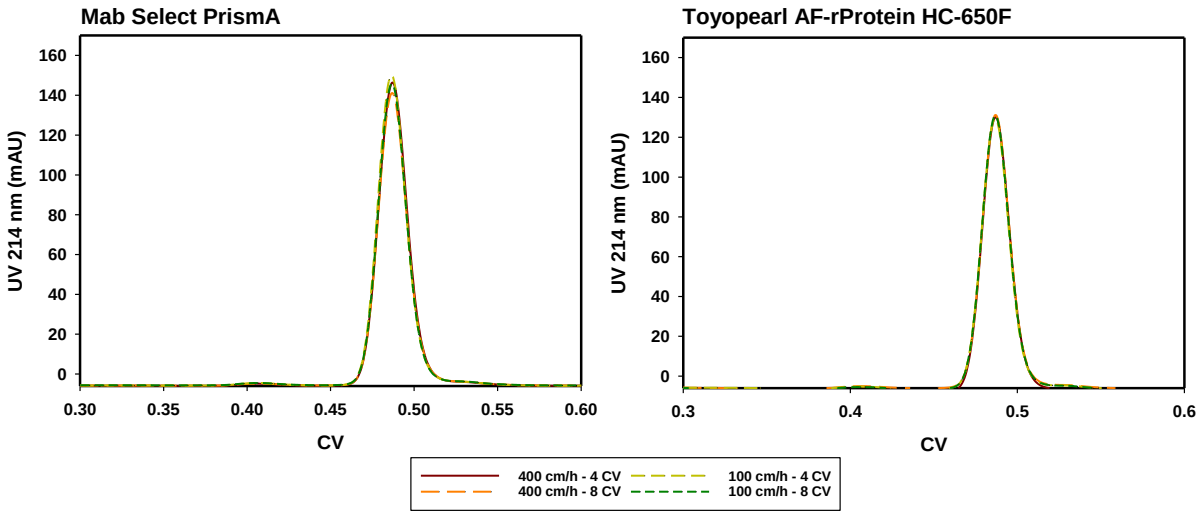

Figure 40: Comparison of SEC results from obtained eluates from the intermediate wash

Figure 41 depicts the impact of the intermediate wash step on the HCP content. For Mab Select PrismA the HCP content could be significantly reduced by one third. This indicates that the intermediate wash buffer succeeded in weakening the mAb-HCP interactions which are described in various studies [27, 32]. One paper showed higher reduction factors for agarose-based resins but the HCP value for MabSelect PrismA eluates in this study is already rather low, therefore it seems difficult to achieve further reduction. Even though this wash buffer was developed and tested on agarose-based resins, the effect on Toyopearl AF-rProtein A HC-650F was tremendous. Overall a reduction of HCP by a factor 50 to 100 could be achieved. This indicates that there are also many specific HCP-resin interactions taking place. The washing velocity and intensity did not show any change of the effect for both resins.

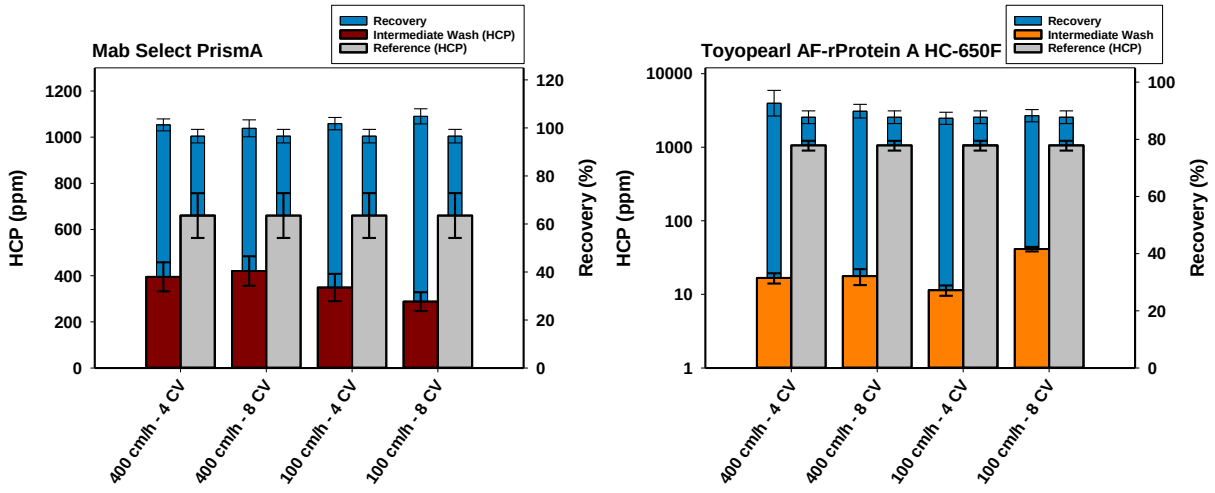

Figure 41: HCP content and recovery of obtained fractions from intermediate wash experiments compared to a reference which has the same conditions excluding the washing step

4 Summary and conclusion

The objective of this work was to compare two high-capacity Protein A resins, Mab Select PrismA from *GE Healthcare* and Toyopearl AF-rProtein A HC-650F from *Tosoh Bioscience*, with special emphasis on effects related to velocity, e.g. the speed of operation. The perspective of this work was related to possible future application of a Protein A affinity membrane device which are currently under development at Sartorius. As such it is useful to gain knowledge on velocity-related effects in Protein A affinity chromatography because the membrane will be operated at very high velocities compared to particulate resins. In the course of this study, following operating parameters were determined: dynamic binding capacity; variation of elution buffers; variation of loading (saturation) and loading velocity; variation of elution velocity; implementation of a pre-elution step and of an intermediate washing step and their impact at different velocities. All eluates were investigated for protein recovery, aggregate formation and HCP content.

The determination of the dynamic binding at 10 % breakthrough capacity yielded very high values of ~ 70 mg/mL at residence times > 6 min for both resins. Effective pore diffusion coefficients were comparably small with values of 1.7 $*10^{-8}$ cm^2/s for MabSelect PrismA and 1.25 $*10^{-8}$ cm^2/s for the Toyopearl resin. Nevertheless, both resins show relatively fast mass transfer over a wide velocity range since the low diffusion coefficient is compensated by the small particle diameters of 60 and 45 µm, respectively. On the other hand, this leads to high pressure drops which restrict to use high velocities and also special care is necessary during alkaline regeneration which has to be performed at very low flow rates to avoid exceeding the pressure limit.

Different elution buffer species and pH values did not show any effect on HCP concentration in the eluate nor aggregate formation of the mAb. However, the latter fact is mainly due to the exceptional stability of the used mAb thus aggregate formation could not be studied properly for the different process conditions. In general, eluates from Mab Select PrismA had a lower HCP content than those purified with Toyopearl AF-rProtein A HC-650F. Furthermore, higher elution velocity lead to slightly broader elution peaks but did not show any impact on the results in terms of HCP values and aggregate formation.

In contrast, the amount of loaded material in combination with the velocity of sample application had a significant impact. Higher HCP levels were obtained at higher velocities, which in turn corresponded to lower saturation. This trend was much more pronounced for Toyopearl AF-rProtein A HC-650F which might be due to increased HCP-resin interaction.

Recovery of mAb in eluates were ~ 85-90% in most relevant cases. Only at low resin saturation recoveries very lower, especially for Toyopearl AF-rProtein A HC-650F.

Introduction of a pre-elution step with a slightly acidic buffer did not show improvements in HCP content in eluates as it was shown by other studies. It has been suggested for other mAbs that such a pre-elution step could reduce aggregate formation as the pH transition from neutral to acidic pH is not so strong. As there was no aggregate formation detected with this

particular mAb, this effect could not be studied and consequently also the velocity dependence could not be assessed.

The implementation of an intermediate wash step with a buffer containing urea and isopropanol yielded a significant reduction of the HCP content for both resins. The investigated washing procedure was originally developed for agarose-based resins, and it showed a HCP reduction of about one third on Mab Select PrismA. Surprisingly, this washing procedure showed an extremely high reduction of the HCP content on the methacrylate resin, where the HCP content could be reduced by a factor of 50 to 100. This indicates that there is definitely a HCP-resin interaction taking place, and that this effect is different for both resins. It is supposed that mAb-HCP interactions are mostly dependent on the mAb itself, therefore it can be suggested that in this case, the HCP-resin interactions are the dominating interactions, as the washing procedure shows different effects on the different resins. It can be assumed that various stationary phases might require specific washing procedures. Furthermore, it is questionable to which extent or if the stationary phase of the resin influences mAb-HCP interactions. Furthermore, the observed reduction effects were not dependent on the washing velocity or on the amount of washing agent used for the washes. The recoveries obtained in these experiments were not influenced noticeable, which underlines the strong and specific binding of protein A to the mAb. Independency on velocity is also a very favourable factor considering future application of Protein A membrane chromatography.

5 References

1. Michael T. Madigan, J.M.M., David A. Stahl, David P. Clark, *Brock Biology of Microorganisms*. 13 ed. 2012.
2. Jungbauer, G.C.a.A., *Protein Chromatography_ Process Development and Scale-Up*. 2010: Wiley, John & Sons.
3. Strohl, W.R.S.a.L.M., *Therapeutic antibody engineering - Current and future advances driving the strongest growth area in the pharmaceutical industry*. 2012: Woodhead publishing series in Biomedicine.
4. AMSBIO. 2018; Available from: http://www.amsbio.com/antibodies-secondary-antibodies.aspx.
5. Ghosh, R., *Protein separation using membrane chromatography: opportunities and challenges.* Journal of Chromatography B, 2002. **952**: p. 13-27.
6. Grilo, A.L. and A. Mantalaris, *The Increasingly Human and Profitable Monoclonal Antibody Market.* Trends Biotechnol, 2018.
7. Liu, J.K., *The history of monoclonal antibody development - Progress, remaining challenges and future innovations.* Ann Med Surg (Lond), 2014. **3**(4): p. 113-6.
8. Krapp, S., et al., *Structural Analysis of Human IgG-Fc Glycoforms Reveals a Correlation Between Glycosylation and Structural Integrity.* Journal of Molecular Biology, 2003. **325**(5): p. 979-989.
9. Matsumiya, S., et al., *Structural comparison of fucosylated and nonfucosylated Fc fragments of human immunoglobulin G1.* J Mol Biol, 2007. **368**(3): p. 767-79.
10. Schroeder, H.W., Jr. and L. Cavacini, *Structure and function of immunoglobulins.* J Allergy Clin Immunol, 2010. **125**(2 Suppl 2): p. S41-52.
11. Zemlin, M., et al., *Expressed Murine and Human CDR-H3 Intervals of Equal Length Exhibit Distinct Repertoires that Differ in their Amino Acid Composition and Predicted Range of Structures.* Journal of Molecular Biology, 2003. **334**(4): p. 733-749.
12. Edry, E. and D. Melamed, *Class switch recombination: a friend and a foe.* Clin Immunol, 2007. **123**(3): p. 244-51.
13. Gad, S.C., *Pharmaceutical Sciences Encyclopedia: Drug Discovery, Development and Manufacturing*. 2010: John Wiley & Sons.
14. Kuo, C.C., et al., *The emerging role of systems biology for engineering protein production in CHO cells.* Curr Opin Biotechnol, 2018. **51**: p. 64-69.
15. Raymund C. Duhamel, P.H.S., Klaus Brendel and Elias Meezan, *pH gradient elution of human IgG1, IgG2 and IgG4 from protein A-sepharose.* Journal of Immunological Methods, 1979. **31**: p. 211-217.
16. Lars Abrahmsen, T.M., Bjorn Nilsson,Ulf Hellman and Mathias Uhlen, *Analysis of signals for secretion in the staphylococcal protein A gene.* The EMBO Journal, 1985. **4**: p. 3901-3906.
17. Tomas Moks, L.A., Björn Nilsson, Ulf Hellman, John Sjöquist and Mathias Uhlen, *Staphylococcal protein A consists of five IgG-binding domains.* European Journal of Biochemistry, 1986. **156**: p. 637-643.
18. Bengt Guss, M.U., Björn Nilsson, Martin Lindberg, John Sjöquist, and Jörgen Sjödahl, *Region X, the cell-wall-attachment part of staphylococcal protein A.* European Journal of Biochemistry, 1984. **138**: p. 413-420.

19. Hober, S., K. Nord, and M. Linhult, *Protein A chromatography for antibody purification.* J Chromatogr B Analyt Technol Biomed Life Sci, 2007. **848**(1): p. 40-7.
20. Pabst, T.M., et al., *Engineering of novel Staphylococcal Protein A ligands to enable milder elution pH and high dynamic binding capacity.* J Chromatogr A, 2014. **1362**: p. 180-5.
21. Watanabe, H., et al., *Structure-based histidine substitution for optimizing pH-sensitive Staphylococcus protein A.* J Chromatogr B Analyt Technol Biomed Life Sci, 2013. **929**: p. 155-60.
22. Li, Y., *Effective strategies for host cell protein clearance in downstream processing of monoclonal antibodies and Fc-fusion proteins.* Protein Expr Purif, 2017. **134**: p. 96-103.
23. Gutierrez, A.H., L. Moise, and A.S. De Groot, *Of [Hamsters] and men: a new perspective on host cell proteins.* Hum Vaccin Immunother, 2012. **8**(9): p. 1172-4.
24. Robert, F., et al., *Degradation of an Fc-fusion recombinant protein by host cell proteases: Identification of a CHO cathepsin D protease.* Biotechnol Bioeng, 2009. **104**(6): p. 1132-41.
25. Gao, S.X., et al., *Fragmentation of a highly purified monoclonal antibody attributed to residual CHO cell protease activity.* Biotechnol Bioeng, 2011. **108**(4): p. 977-82.
26. Agency, E.M. *ICH Q6B Specifications test procedures and acceptance criteria for biotechnologicalbiological products*. 1999 [cited 2018; Available from: http://www.ema.europa.eu/ema/index.jsp?curl=pages/regulation/general/general_content_000883.jsp&mid=WC0b01ac058002956b.
27. Goey, C.H., S. Alhuthali, and C. Kontoravdi, *Host cell protein removal from biopharmaceutical preparations: Towards the implementation of quality by design.* Biotechnol Adv, 2018. **36**(4): p. 1223-1237.
28. Nicholas E. Levy, K.N.V., Leila H. Choe, Kelvin H. Lee, Abraham M. Lenhoff, *Identification and Characterization of Host Cell Protein Product-Associated Impurities in Monoclonal Antibody Bioprocessing.* Biotechnology and Bioengineering, 2014. **111**: p. 904-912.
29. Lintern, K., et al., *Residual on column host cell protein analysis during lifetime studies of protein A chromatography.* J Chromatogr A, 2016. **1461**: p. 70-7.
30. Abhinav A. Shukla, C.J., Junfen Ma, Michael Rubacha, Lisa Flansburg, and and S.S. Lee, *Demonstration of Robust Host Cell Protein Clearance in Biopharmaceutical Downstream Processes.* Biotechnology Progress, 2008. **24**: p. 615-622.
31. Tarrant, R.D., et al., *Host cell protein adsorption characteristics during protein A chromatography.* Biotechnol Prog, 2012. **28**(4): p. 1037-44.
32. Hinckley, A.A.S.a.P., *Host Cell Protein Clearance During Protein A Chromatography: Development of an Improved Column Wash Step.* Biotechnology Progress, 2008. **24**: p. 1115-1121.
33. Hahn, R., *Methods for characterization of biochromatography media.* J Sep Sci, 2012. **35**(22): p. 3001-32.
34. Pabst, T.M., J. Thai, and A.K. Hunter, *Evaluation of recent Protein A stationary phase innovations for capture of biotherapeutics.* J Chromatogr A, 2018. **1554**: p. 45-60.
35. Roque, A.C., C.S. Silva, and M.A. Taipa, *Affinity-based methodologies and ligands for antibody purification: advances and perspectives.* J Chromatogr A, 2007. **1160**(1-2): p. 44-55.
36. Ayyar, B.V., et al., *Affinity chromatography as a tool for antibody purification.* Methods, 2012. **56**(2): p. 116-29.
37. Yang, L., et al., *Effect of cleaning agents and additives on Protein A ligand degradation and chromatography performance.* J Chromatogr A, 2015. **1385**: p. 63-8.

38. Rainer Hahn, R.S., Alois Jungbauer, *Comparison of protein A affinity sorbents.* Journal of Chromatography B, 2003. **790**: p. 35-51.
39. Hahn, R., et al., *Comparison of protein A affinity sorbents II. Mass transfer properties.* J Chromatogr A, 2005. **1093**(1-2): p. 98-110.
40. Orr, V., et al., *Recent advances in bioprocessing application of membrane chromatography.* Biotechnol Adv, 2013. **31**(4): p. 450-65.
41. Olivier P. Dancette, J.-L.T., Eric Tournier, Catherine Charcosset, Pierre Blond, *Purification of immunoglobulins G by protein A/G affinity membrane chromatography.* Journal of Chromatography B, 1999. **723**: p. 61-68.
42. Madadkar, P. and R. Ghosh, *High-resolution protein separation using a laterally-fed membrane chromatography device.* Journal of Membrane Science, 2016. **499**: p. 126-133.
43. Ghosh, R., P. Madadkar, and Q. Wu, *On the workings of laterally-fed membrane chromatography.* Journal of Membrane Science, 2016. **516**: p. 26-32.
44. Etzel, S.-Y.S.a.M.R., *A mathematical analysis of affinity membrane bioseparations.* Chemical Engineering Science, 1992. **47**: p. 1355-1364.
45. Sadavarte, R., et al., *Rapid preparative separation of monoclonal antibody charge variants using laterally-fed membrane chromatography.* J Chromatogr B Analyt Technol Biomed Life Sci, 2018. **1073**: p. 27-33.
46. Vikram N. Sisodiya, J.L., Maricel Rodriguez, Paul McDonald and Kathlyn P. Lazzareschi, *Studying host cell protein interactions with monoclonal antibodies using high throughput protein A chromatography.* Biotechnology Journal, 2012. **7**: p. 1233-1241.
47. Perchiacca, J.M. and P.M. Tessier, *Engineering aggregation-resistant antibodies.* Annu Rev Chem Biomol Eng, 2012. **3**: p. 263-86.
48. Lowe, D., et al., *Aggregation, stability, and formulation of human antibody therapeutics.* Adv Protein Chem Struct Biol, 2011. **84**: p. 41-61.
49. Shukla, A.A., P. Gupta, and X. Han, *Protein aggregation kinetics during Protein A chromatography: Case study for an Fc fusion protein.* Journal of Chromatography A, 2007. **1171**(1): p. 22-28.
50. Roberts, C.J., *Protein aggregation and its impact on product quality.* Curr Opin Biotechnol, 2014. **30**: p. 211-7.

6 Appendix

6.1 List of figures:

6.2 List of equations:

6.3 List of tables: